RESEARCH

Effect of Thermal and Non-thermal Plasma Treatment on Particle Size Distribution, Protein Secondary Structure, Fuzzy Logic Sensory Evaluation, Rheological, and Selected Quality Attributes of Pineapple Juice: A Comparative Analysis

Sunil Pipliya[1] · Sitesh Kumar[1] · Prem Prakash Srivastav[1]

Abstract

This study presents the comparative analysis of untreated, optimized non-thermal plasma (NTP)–treated (38 kV/631 s), extreme NTP–treated (45 kV/900 s), and thermally treated (95 °C/12 min) pineapple juice (PJ) on enzyme activity, microbial count, protein structure, particle size, bioactive substances and, sensory, rheological, and biochemical attributes. The PJ treated with optimized NTP demonstrated merits over extreme NTP–treated and thermally treated in terms of the retention of bromelain, bioactive components, and biochemical attributes. Moreover, the fuzzy logic evaluation showed that optimized NTP–treated juice had superior sensory characteristics than extremely NTP– and thermally treated juice. The NTP approach, like thermal treatment (95 °C/12 min), extends shelf life by assuring microbiological safety ($<1 \log_{10}$ cfu/mL) and enzyme inactivation ($>90\%$). However, the thermal treatment resulted in loss of bioactive, sensory, and biochemical attributes. Particle size distribution indicates that NTP significantly ($p < 0.05$) reduced the sauter mean and volume mean diameter from 1617 to 894 nm and 1688 to 917 nm, respectively, which stabilized juice after treatment. NTP treatment substantially reduced the consistency from 1.22 to 0.31 mPa.s^n and showed a pseudo-plastic behavior of juice. These results collectively imply that NTP has a tremendous ability to maintain bioactive compounds, and sensory and physicochemical attributes, as well as extend the shelf life of PJ.

Keywords Non-thermal plasma · Fuzzy logic · Thermal treatment · Rheological properties · Pineapple juice

Introduction

Pineapple is a tropical fruit native to South America, now cultivated in many countries worldwide. It is a member of the Bromeliaceae family, and its scientific name is *Ananas comosus* L. The pineapple fruit has a tough, spiky outer skin, usually brown or yellow. The fruit's interior is composed of juicy, yellow flesh with a sweet and tangy flavor. Pineapple is an abundant source of vitamin C, manganese, and a small amount of other vitamins and minerals. It can be consumed fresh, canned, or juiced and is a popular ingredient in many dishes, including pizza, salads, and smoothies. Among the processed pineapple products, pineapple juice (PJ) is a ubiquitous and refreshing beverage extracted from pineapple, with a distinct tangy and sweet flavor. It is famous for its attractive aroma, revitalizing taste, health benefits, and adaptability in various culinary applications (Laorko et al., 2013).

Because it contains higher vitamin C, sugar, dietary fiber, micronutrients, and phenolic compounds, PJ experiences greater consumer acceptability, it also provides other vital vitamins and minerals like vitamin B$_6$, manganese, potassium, and calcium. PJ includes a variety of phenolic and antioxidant substances (carotenoids, phenolic, flavonoids, and vitamin C) that may have several health advantages and

✉ Sitesh Kumar
siteshkumar27@yahoo.com

Sunil Pipliya
sunilpipliya22@gmail.com

Prem Prakash Srivastav
pps@agfe.iitkgp.ac.in

1   Food Science and Technology Laboratory, Department of Agricultural and Food Engineering, Indian Institute of Technology Kharagpur, Kharagpur 721302, West Bengal, India

a preventive action against disease (Pipliya et al., 2022). Vitamin C, an antioxidant vital to immune system function, skin health, and wound healing, is abundant in PJ.

PJ is seasonal and highly perishable regardless of having nutritional and physiological advantages. Fulfilling consumer demand for this product might be threatened by PJ's shortened life span due to microbial and enzymatic deterioration. In order to produce safe and stable PJ with an extended shelf life, conventional thermal treatment (pasteurization) is the preferred method over other techniques. However, this method adversely impacts the nutritional, physicochemical, and sensory quality attributes of juice after processing (Wurlitzer et al., 2019). Minimally processed food products have gained popularity in recent years as a result of consumer expectations for foods of superior quality with "fresh-like" and additive-free characteristics that need minimal effort and time to prepare. Therefore, to fulfill these demands, various novel non-thermal technologies, including high hydrostatic pressure processing, pulsed electric field, UV treatment, and gamma irradiation, have been utilized in the food sector for juice processing (Kumar et al., 2023b). These methods have demonstrated their superiority in preserving the sensory and organoleptic qualities of fruits and vegetables. Additionally, they effectively deactivate enzymes and decontaminate microbes (Wu et al., 2020). Nonetheless, there exist certain constraints while implementing these non-thermal methods. These include intricacies in their application, the substantial construction expenses involved, negative perceptions, and challenges tied to scaling up these approaches. As a result, to counter these limitations, non-thermal plasma (NTP) techniques have emerged as a compelling substitute for effectively inactivating foodborne pathogens (Pipliya et al., 2023a; Wang et al., 2020; Ziuzina et al., 2014), some enzyme inactivation (Illera et al., 2019; Xu et al., 2017), and better retention of food quality characteristics (Kumar et al., 2023a) by eliminating the requirement of any chemical agent (additives and preservatives) at ambient temperatures condition. Though there is a minor rise in temperature during NTP treatment, this temperature rise is inadequate to degrade the nutritional compounds present in food (Pipliya et al., 2023c).

The current research in the field of NTP encompasses several investigations pertaining to pathogenic enzymes (Miguel et al., 2021; Wu et al., 2023), rheological and structural analysis (da Costa Pinto et al., 2023; Nasiru et al., 2023; Zielinska et al., 2022), packaging films (Rashvand et al., 2023), pre-treatment methods in the drying and extraction process (Ashtiani et al., 2023; Karunanithi et al., 2022; Li et al., 2023; Mehta et al., 2022; Namjoo et al., 2022), and analysis of volatile composition and physicochemical properties of juice (Alves Filho et al., 2021; Kalaivendan et al., 2023; Rodrigues & Fernandes, 2023), as well as the study of food allergies (Cheng et al., 2023; Feizollahi &

Roopesh, 2021; Sharma et al., 2022). There is a scarcity of research that examines the comparison between NTP-treated juice and thermally treated juice in terms of parameters such as particle size, rheology, juice acceptability, and physicochemical properties. The primary objective of the present study is to fill the void in the existing literature.

Materials and Methods

Chemical and Reagents Required

Trichloroacetic acid, sodium chloride, 2,2-Diphenyl-1-picrylhydrazyl, pyrogallol, ascorbic acid, meta-phosphoric acid, hydrogen peroxide, aluminum chloride, azocasein, catechol, disodium hydrogen phosphate, quercetin, sodium nitrite, gallic acid, Folin–Ciocalteu reagent, potassium dihydrogen phosphate, and sodium carbonate were bought from Merck Specialities Pvt. Ltd., India, whereas plate count agar, polyvinylpolypyrrolidone (PVPP), Triton-X-100, and yeast and malt agar were procured from Himedia Laboratories Pvt. Ltd., India. All reagents and chemicals needed for the food quality analysis were of analytical grade.

Sample Preparation for Treatment

Pineapples (*Ananas comosus L. Cv. Queen*) with a pleasing aroma and flavor were acquired from a local marketplace nearby the Indian Institute of Technology Kharagpur, India. The obtained fruits were adequately washed using soft water, and their surfaces were disinfected by submerging them in a 100 ppm sodium hypochlorite solution for a duration of 3 min. Following the disinfection process, the fruit underwent an extensive rinse using distilled water and was gently dried to remove any remaining traces of chlorine (Chakraborty et al., 2015b). Furthermore, the eye, skin, and core were meticulously separated from the fruit through a high-quality stainless-steel knife, and the remaining edible part was cut into small slices. The puree was produced by uniformly mixing the cut pineapple slices at 6000 rpm for 5 min in a household fruit juicer. Before collection, the puree was filtered to obtain juice via a 3-layer muslin cloth. The sample was sealed in glass bottles and stored at $-35\,°C$ until it was utilized again for experimentation.

NTP Setup and Treatment

Figure 1 illustrates the schematic depiction of the dielectric barrier discharge (DBD) plasma setup. The high-voltage DBD plasma system (model no. Z/45/14), procured from Zeonics Systech Defence and Aerospace Engineers Private Limited, India, encompasses essential components such as power cords, a high-voltage (HV) connector, a voltage
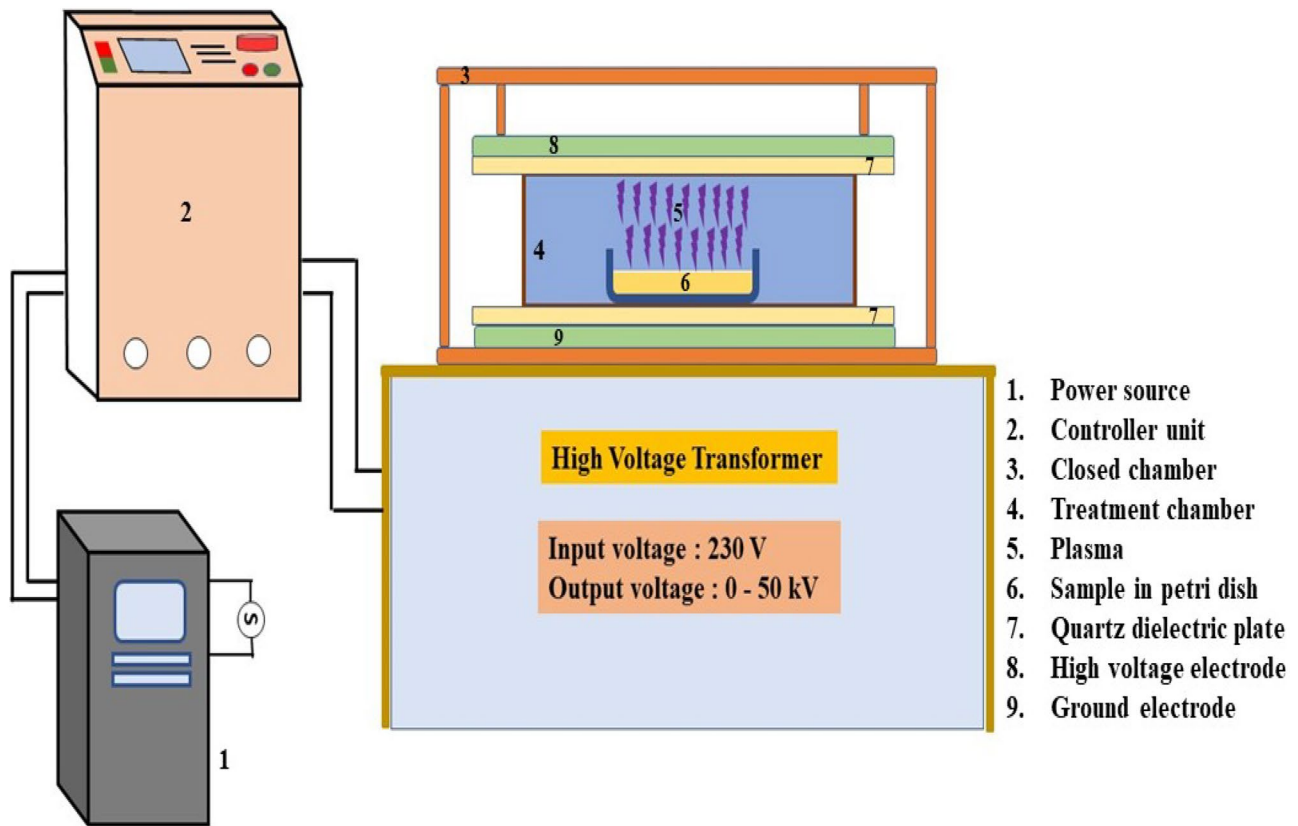
Fig. 1 Schematic representation of dielectric barrier discharge non-thermal plasma system

regulator, and the treatment chamber. The treatment chamber is constructed with 5-mm thickened two parallel copper electrodes that are positioned 15 mm apart, encompassing an area of 1225 cm^2. These electrodes are further enclosed by 3-mm-thick quartz plates, serving as the dielectric barrier. The power input to the primary coil of the step-up transformer is 230 V from a 50 Hz. The upper electrode is linked to a high-voltage generator capable of producing voltages of up to 50 kV (2500 W) at 50 Hz, while the lower electrode remains grounded. The pineapple juice was kept in Petri dish at depth of 8 mm and exposed to two different treatment conditions, viz. optimized and extremely NTP treatment. The parameters for optimized (38 kV/631 s, S2) and extremely (45 kV/900 s, S3) NTP treatment were selected from already published research article (Pipliya et al., 2023b).

Thermal Treatment

As part of the thermal pasteurization process, the PJ was treated at 55 °C, 65 °C, 75 °C, 85 °C, and 95 °C for a duration of 12 min in a temperature-controlled (± 0.5 °C) water bath (RWBS, Reico Equipment & Instrument Pvt. Ltd). The countdown timer for treatment commenced once the center of sample reached the desired temperature. After the thermal treatment, the juice was rapidly cooled down using an ice bath. The temperature of the juice within the beaker was measured using thermocouples, providing a precision of 1 °C throughout the duration of the experiment. The treatment condition was selected on the basis of a 5 log cycle decrease in the target microorganisms in the juice sample and about 90% inactivation in the activity of resistant enzymes such as polyphenol oxidase and peroxidase (Chakraborty et al., 2015b).

Measurement of pH, Titratable Acidity (TA), and Total Soluble Solid (TSS)

Ranganna (2007) described the method for determination of pH, TSS, and TA of PJ samples. The pH of the juice samples was measured using a digital pH meter (model: CL 46+ ; manufacturer: Toshcon, India), while the total soluble solids (TSS) were determined using a handheld refractometer (model: PAL-1; manufacturer: Atago, Japan). The juice sample's acidity was determined as grams of citric acid per 100 mL of juice through titration against a sodium hydroxide solution. The TSS content of the samples was measured in °Brix.

Measurement of Color

The color of the juice samples before and after NTP treatment was assessed on the principle of the CIE colorimeter (KONIKA MINOLTA, Japan) scale, where $a*$ (red to green), $b*$ (yellow to blue), and $L*$ (lightness) were measured in the 3D domain, respectively. Black and white tiles that were given were used to calibrate the colorimeter. The total color change ($\Delta E*$) examined the difference in color between the control and NTP-treated samples (Kumar et al., 2023a). The total color change ($\Delta E*$) of NTP-treated juice samples was quantified by the following Eq. (1):

$$\Delta E = \sqrt{(L_1^* - L_2^*)^2 + (a_1^* - a_2^*)^2 + (b_1^* - b_2^*)^2} \quad (1)$$

where subscripts "1" and "2" show the $L*$, $a*$, and $b*$ values of control NTP-treated samples, respectively. Analytically, observed color differences may be divided into three categories: highly different (TCD > 3), distinct (1.5 < TCD < 3), and minor differences (TCD < 1.5).

Determination of Enzyme Activity

Preparation of Crude Enzyme Extract for PPO and POD

The enzyme extraction solution was formulated using 0.2 M Sorenson's phosphate buffer at a pH of 6.5, incorporating 4% (w/v) polyvinylpolypyrrolidone, 1% Triton-X-100, and 1 M sodium chloride. After that, a mixture of 1 mL extraction solution and 1 mL sample was blended, then centrifuged (14,000 rpm) for 25 min at a temperature of 4 °C. The resulting supernatant was utilized for the enzymatic assay.

Enzymatic Assay for PPO and POD

The enzymatic assessment of PPO and POD enzymes was conducted following the procedure outlined by Pipliya et al. (2022). For the PPO assay, the mixture comprised 0.2 mL of enzyme extract, 1.8 mL of 0.1 M catechol, and 1 mL of phosphate buffer with a pH of 6.5. The blank solution was crafted by substituting the sample extract with buffer. The absorbance readings for the PPO assay were recorded at 420 nm for every 10 s over a span of 5 min. As for the POD assay, the mixture was composed of 0.2 mL of enzyme extract within 1.5 mL of SSP buffer, 0.2 mL of 1.5% (v/v) hydrogen peroxide (H_2O_2), and 0.2 mL of guaiacol within 0.05 M SSP buffer. For the blank, the sample extract was exchanged for an SSP buffer. Absorbance measurements for the POD assay were captured every 10 s for a duration of 3 min at a wavelength of 470 nm. The percentage of residual activity (RA) for both PPO and POD enzymes was computed employing Eq. (2):

$$RA\ (\%) = \frac{A_t}{A_o} * 100 \quad (2)$$

Here, A_t represents the residual activity of the juice sample after treatment, while A_o signifies the activity before treatment.

Bromelain Activity

Proteolytic (PRO) activity in pineapple products is the primary measure of bromelain activity. The methodology was slightly modified to measure the PRO activity, and an equation developed by Sew et al. (2014) was used to determine the outcome. For PRO activity, 0.1 mL of juice was added with 2 mL of deionized water and 1 mL of 1% azocasein in phosphate buffer. Following a thorough homogenization, the solution was incubated at 40 °C for 10 min. To halt the reaction, 6 mL of 5% trichloroacetic acid was introduced, leading to the precipitation of non-hydrolysed azocasein. After 5 min of equilibration at ambient temperature (27 °C), the reaction mixture was clarified using Whatman filter paper (Whatman, England). A spectrophotometer was utilized to measure the filtrate's absorbance at 440 nm. The azocasein solution was added to the PJ just before the TCA was added to make the reaction blank. The percentage inactivation of bromelain enzymes was given by following Eq. (3):

$$BRM\ inactivation\ (\%) = \frac{A_o - A_t}{A_o} \quad (3)$$

where the bromelain activity of the control NTP-treated sample in PJ is represented by A_o and A_t.

Measurement of Bioactive Substances in Pineapple Juice

Measurement of Ascorbic Acid (AA) by Titration Method

Ranganna (2007) described the titrimetric approach to determine the ascorbic acid (AA) content in juice samples. A 2, 6-dichlorophenol-indophenol dye solution can be decolored and reduced by ascorbic acid. Meta-phosphoric acid and standard ascorbic acid solutions were titrated against the dye solution until the appearance of the rose-pink color, which provided the dye factor. After that, the juice extract was titrated against the dye solution until the pink endpoint remained for 15 s. The amount of AA in the juice was estimated as mg of AA per 100 mL sample. The reduction in ascorbic acid (AA) content (%) in the NTP-treated sample was determined in comparison to the control sample.

Measurement of Total Phenol Content (TPC) by Folin–Ciocalteu Reagent (FCR) Assay

To assess the total phenolic content and antioxidant capacity, the juice samples were subjected to methanolic extraction. A combination of methanol and the juice sample in a 1:1 (v/v) ratio was prepared, followed by agitation for 30 min at ambient temperature. Subsequently, the mixture was centrifuged at $6000 \times g$ for 15 min at 4 °C to facilitate juice extraction.

The FCR technique reported by Kumar et al. (2023a) was used to quantify the TPC of PJ samples with slight modifications. To conduct the TPC assay, 0.2 mL of the sample extract was combined with 0.5 mL of Folin–Ciocalteu reagent (FCR), 0.75 mL of 20% sodium bicarbonate solution, and the remaining volume was filled with water, resulting in a total volume of 4 mL. This mixture was then incubated at room temperature in the dark for 90 min. Once the mixture had developed a blue color after incubation, its absorbance was measured at 760 nm using a spectrophotometer. The TPC was determined using a calibration curve generated from gallic acid. The TPC of the juice was quantified in milligrams of gallic acid equivalent per 100 mL of the juice sample (mg GAE/100 mL sample).

Measurement of Total Flavonoid Content (TFC)

Flavonoids from the sample were extracted using a solvent mixture of 80% (v/v) methanol in distilled water. To extract the total flavonoid content (TFC), a 5 mL sample was mixed with 20 mL of the solvent and stirred for 2 h at room temperature. Subsequently, the mixture underwent centrifugation for 4 h at 12000 rpm. According to the methodology outlined by Kumar et al. (2023a), the TFC of supernatant was assessed. After mixing the 0.5 mL sample extract with sodium nitrite (5%, 0.15 mL), the mixture was allowed to incubate for 5 min. After the mixture had been incubated, aluminum chloride (0.15 mL, 10%) was added. Further, it was incubated for 5 min before being added to 1 M sodium hydroxide (0.5 mL) and remaining distilled water to make up a volume of up to 4 mL. The alteration in absorbance was measured at 415 nm using quercetin as the reference standard. The TFC was expressed as milligrams of quercetin equivalents (QE) per 100 mL of the juice sample.

Total Antioxidant Capacity (TAC) by 2, 2-Diphenyl-1-Picrylhydrazl (DPPH) Assay

In terms of its capability to scavenge DPPH-free radicals, the methanolic extract of the juice sample's overall antioxidant capacity was evaluated. TAC of extract samples was estimated utilizing the method reported by Igual et al. (2010) with a slight modification. Roughly, 15 mg of DPPH was dissolved in 100 mL of methanol, followed by measuring the absorbance using a spectrophotometer at a wavelength of 517 nm. The DPPH solution's absorbance was adjusted to unity and stored at −20 °C for later use. The addition of juice extract or standard gallic acid with concentrations ranging from 0.1 to 1 mL is primarily responsible for the alteration in DPPH's color from purple to yellow. The TAC assay involved combining 0.2 mL of the sample extract with 0.95 mL of DPPH and 2.85 mL of methanol. This mixture was then incubated in darkness for 30 min. At 517 nm, the mixture's change in absorbance was measured, and the result was represented as the gallic acid equivalent antioxidant capacity (GAEAC) per 100 mL of juice. The percentage of TAC was calculated as Eq. (4):

$$\text{TAC (\%)} = \frac{A_{\text{control}} - A_{\text{sample}}}{A_{\text{control}}} \tag{4}$$

where A_{control} is the absorbance of an untreated sample, and A_{sample} is the absorbance of NTP-treated samples.

Enumeration of Total Microbial Population in Fruit Juice

Yeasts and molds count, and the aerobic mesophiles count group of microorganisms were the two groups for which the survivability count was enumerated by using the serial dilution spread plate technique (Pipliya et al., 2023a). The media for growth used for AM and YM count was nutrient agar and yeast and molds agar, respectively. The incubation environments (temperature and duration) for the Petri plates corresponding to AM and YM count were 37 °C for 24–36 h and 30 °C for 5 days, respectively. Colony-forming units (cfu) were used to quantify the sample's number of colonies expressed as $\log_{10}$ cfu/mL, as shown in Eq. (5).

$$\text{Colony} - \text{forming unit} \left(\frac{\text{cfu}}{\text{mL}}\right) = \frac{\text{No. of colonies in Petri plate} * \text{Total dilution factor}}{\text{Volume of cultured plate in mL}} \tag{5}$$

Particle Size Distribution

The particle size distribution (PSD) analysis of PJ samples was conducted using the Zeta-sizer Nano-ZS90 equipment

manufactured by Malvern Instruments Ltd., UK. Prior to the determination, all samples underwent a dilution process 10 times, as per the method described by Wang et al. (2020). According to Suo et al. (2022a), the utilized parameters encompassed $D_{(4, 3)}$, denoting the volume diameter, which corresponds to the sphere diameter with the equal volume as the particles within the system (Eq. 6). Additionally, $D_{(3, 2)}$ represented the sauter mean or surface diameter, reflecting the average diameter of particles concerning surface area to total volume ratio (Eq. 7). The parameter $D_{(4, 3)}$ is indicative of larger particle presence, whereas $D_{(3, 2)}$ is indicative of smaller particle presence.

$$D_{(4,3)} = \frac{\sum n_i d_i^4}{\sum n_i d_i^3} \tag{6}$$

$$D_{(3,2)} = \frac{\sum n_i d_i^3}{\sum n_i d_i^2} \tag{7}$$

Span values were also computed for all juice samples employing Eq. (8):

$$Span = \frac{D_{(v,0.9)} - D_{(v,0.1)}}{D_{(v,0.5)}} \tag{8}$$

Here, $D_{(v, 0.1)}$ (nm) and $D_{(v, 0.1)}$ (nm) represent the 10th and 90th % particle diameters, respectively, while $D_{(v, 0.5)}$ (nm) stands for the volume median diameter (50th %).

Rheological Analysis

Rheological analyses were carried out utilizing the AR2000 rheometer, employing a cone-plate probe with a diameter of 60 mm. The experimental setup followed the methodology outlined by Huang et al. (2018) with minor adjustments. A volume of 0.5 mL of juice samples was transferred onto the bottom plate. According to Wei and Ren (2018), steady-state flow analysis was conducted within a shear rate range of 0.1 to 100 s^{-1}. An incubation period of 3 min on the plate was implemented for the juice samples prior to each analysis. In the subsequent dynamic frequency sweep analysis, a strain of 2% was selected following the strain sweep experiments. The behavior of the loss modulus (G″) and storage modulus (G′) was assessed over a frequency range spanning from 0.1 to 10 Hz (Wei & Ren, 2018). The analysis of the rheological data was facilitated by employing the rheology advantage software. The flow characteristics of the juice samples were described employing the Herschel Bulkley model (Eq. 9).

$$\tau = \tau_0 + K.\gamma^n \tag{9}$$

Here, τ represents the shear stress (mPa), τ_0 represents the yield stress (mPa), γ represents the shear rate (s^{-1}), k represents the consistency index (mPa*s^n), and n represents the flow behavior index of the sample.

Secondary Structure of a Protein by Fourier-Transform Infrared Spectroscopy (FTIR) Peak Deconvolution

The secondary structure of PJ protein was analyzed by an FTIR spectrometer. The obtained spectra underwent Fourier self-deconvolution, second derivative analysis, and curve fitting procedures. These steps were utilized to identify and distinguish overlapping peaks within the Amide-I region (1600–1700 cm^{-1}) (Shevkani et al., 2015). The analysis was conducted using peak deconvolution application in origin 10.05.157. Quantifying the relative proportions of distinct secondary structures in PJ was accomplished by calculating the areas of spectral components (Gaussian peaks) attributed to specific substructures within the Amide-I region.

Fuzzy Logic Sensory Evaluation

Selection and Training of Panelists

A sensory panel comprising 13 participants was selected from a cohort of 25 research scholars associated with the Department of Agricultural and Food Engineering at the Indian Institute of Technology Kharagpur. These individuals, aged between 23 and 35 years, were non-smokers, possessed no allergy to pineapple, and exhibited a keen interest in sensory testing. The selected panel members underwent comprehensive training in various sensory analysis procedures. They received education about recognizing and comprehending various errors and external influences that could potentially impact the integrity of sensory analysis. The objective of this training was to mitigate the influence of biases, stimulus errors, and psychological factors such as habituation, ensuring the integrity of the evaluation process. They were thoroughly educated on proper sampling techniques and the correct interpretation of responses through appropriate scoring methods tailored to each kind of sensory evaluation. Panel members were instructed to immediately inform about any health concerns, like cold, fever, or other conditions that could impact their sense of smell. Panelists were given comprehensive instructions about the scorecard and the methods for assigning scores. The concepts of score values and their representation within a score range were explained to ensure a clear understanding of how to translate their perceptions into numerical scores.

Sensory Evaluation

Incorporating fuzzy logic into sensory analysis involves transforming the data collected from panel members' responses,

which often encompass imprecise observations. These responses are then subjected to mathematical interpretation, which is analyzed as membership functions (MF). These functions act as representations of the panel members' non-numeric sensory perceptions. The MF utilized in this sensory study is classified as triangular. This selection aligns with its ability to represent the predetermined set of sensory responses effectively. The quality attributes for sensory analysis included aspects such as color (C), taste (T), mouthfeel (M), aroma (A), and aftertaste (AT). The scale used for evaluation encompassed descriptors such as "Not satisfactory," "Fair," "satisfactory," "Good," "Very good," and "Excellent," represented on a fuzzy scale. The implementation of this approach utilized Microsoft Excel 2016 for its execution.

PJ sample preferences were determined using a triangular fuzzy MF. The sensory scores attributed to the juice samples by the panelists, employing fuzzy scores, were transformed into sets of triplets. Subsequently, a similarity analysis was conducted to establish sample rankings (Vivek et al., 2020). The triplets were labeled as "(a b c)," with "a" indicating a point on the horizontal axis of the MF where the vertical axis value is 1. "b" indicates the distance to the left of "a" where the vertical value is zero, and "c" indicates the distance to the right of "a" where the vertical value is zero. The pattern of distribution of 5-point sensory scales includes the following categories: "Not satisfactory/Not at all important" with values (0, 0, 25), "Fair/Somewhat important" with values (25, 25, 25), "Medium/Important" with values (50, 25, 25), "Good/Highly important" with values (75, 25, 25), and "Excellent/Extremely important" with values (100, 25, 0), as shown in Fig. 2a. As an illustration, for the color (C) of sample S1, the opinions of the panelists were as follows: 0
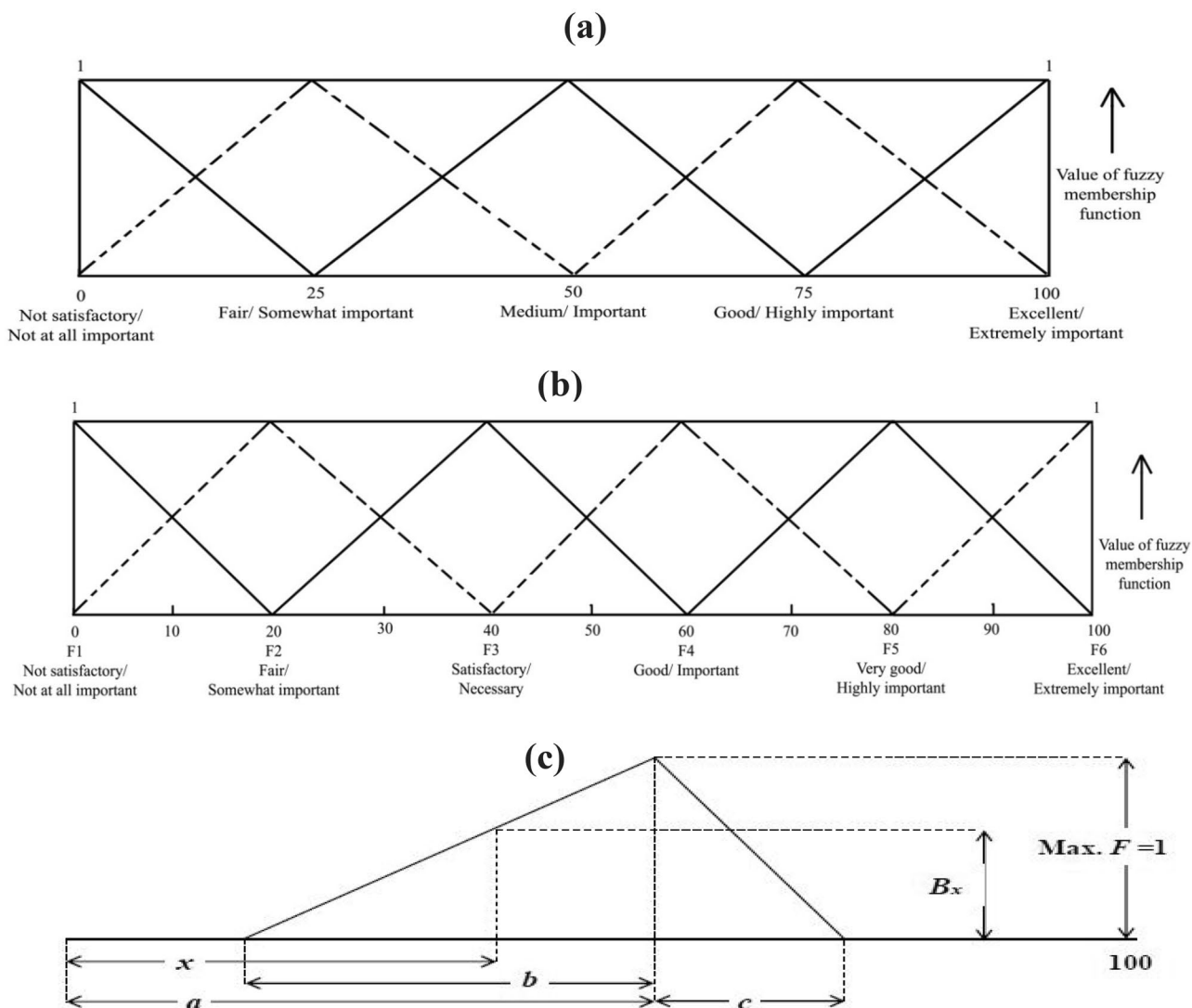

Fig. 2 Overview of fuzzy logic sensory evaluation; **a** representation of triangular membership function distribution pattern of sensory scales; **b** standard fuzzy scale; **c** representing the triplets of the sensory score (a b c) into the membership function

rated it as "poor," 0 rated it as "fair," 4 rated it as "good," 6 ranked it as "very good," and 3 rated it as "excellent." These sensory scores were converted into corresponding triplets for sample S1, as depicted in Eq. (10).

$$S1C = \frac{0(0\ 0\ 25)\ +\ 0(25\ 25\ 25)\ +\ 4(50\ 25\ 25)\ +\ 6(75\ 25\ 25)\ +\ 3(100\ 25\ 0)}{(0\ +\ 0\ +\ 4\ +\ 6\ +\ 3)} = (73.07\ 25\ 19.23) \quad (10)$$

The exact methodology was employed to compute the triplet of samples for all quality attributes and a triplet of sensory attributes of PJ in general. Additionally, a relative weightage triplet (QC_{rel}) was determined for the sensory quality characteristics in general terms by calculating the ratio of each individual triplet to the greatest value among the total of the triplet sides. The overall sensory score (SO_i) for the ith sample was determined using Eq. (11).

$$SO_i = \sum_{j=1}^{5} (S_i \text{ for } j\text{th attributes}) \times (QC_{rel} \text{ for } j\text{th attributes}) \quad (11)$$

In this context, the variable "j" denotes the sensory attributes being analyzed: color, aroma, taste, mouthfeel, and aftertaste. Each characteristic is assigned a value of 1 to 5, according to its respective order in the sequence. The multiplication among the triplets was performed using the methodology outlined by Basak (2018). The MF denoted as F1 to F6, based on the linguistic expression standard fuzzy scale, are expressed in Table S1, whereas the standard fuzzy scale, which adheres to a triangular distribution pattern of a 6-point sensory scale, is depicted in Fig. 2b. The MF for the overall sensory scores of PJ samples was determined using the standard fuzzy scale. As depicted in Fig. 2c, when the abscissa value is denoted as "a," the MF's value becomes 1. Additionally, within the range of abscissa values from (a − b) to (a + c), the MF's value transitions to 0. Given a specific value of "x" on the abscissa, the value of the MF, denoted as B_x, can be formulated as follows (Eqs. 12–14):

$$B_x = \frac{x - (a - b)}{b} \text{ for } (a - b) < x < a \quad (12)$$

$$B_x = \frac{(a + c) - x}{c} \text{ for } a < x < (a + c) \quad (13)$$

$$B_x = 0 \text{ for all other values of } x \quad (14)$$

MF values, denoted as B_x, were computed for each sample at specific points along the abscissa: $x = 0, 10, 20, 30, 40, 50, 60, 70, 80, 90,$ and 100.

Once the MF of each juice sample was determined, a comparison was made between the similarity values of these samples and the corresponding values of the MF within the standard fuzzy scale. Subsequently, similarity values were calculated for each sample under categories F1 (Not satisfactory), F2 (Fair), F3 (Satisfactory), F4 (Good), F5 (Very good), and F6 (Excellent). This calculation was carried out using the following Eq. (15):

$$S_m(F, B) = \frac{F \times B^T}{\text{maximum of } (F \times F^T \text{ and } B \times B^T)} \quad (15)$$

In this context, the similarity value for a specific sample, denoted as "S_m," was calculated. The term "$F \times B^T$" represents the matrix product of matrix F with the transpose of matrix B, while "$F \times F^T$" stands for the matrix product of matrix F with its own transpose. Furthermore, "$B \times B^T$" signifies the matrix product of matrix B with its transpose. For instance, for sample 1, the calculation of similarity values, namely Sm (F1, B1), Sm (F2, B1), Sm (F3, B1), Sm (F4, B1), Sm (F5, B1), and Sm (F6, B1), was conducted through the principles of matrix multiplication.

Statistical Analysis

The obtained data was statistically analyzed using SPSS 29.0 software developed by IBM Inc. in Armonk, NY, USA. The data in this investigation were represented as mean ± standard deviations. The research utilized a one-way analysis of variance (ANOVA) in combination with Tukey's honestly significant difference (HSD) test. This approach was employed to detect statistical change ($p < 0.05$) in the average values among various PJ samples. The figures were produced using the Origin 2023 software.

Results and Discussion

Thermal Treatment of Pineapple Juice

Effect on Aerobic Mesophiles and Yeasts and Molds Count

The aerobic mesophiles microbial population was measured to be 5.12 $\log_{10}$ cfu/mL, while the count for yeasts and molds was 4.53 $\log_{10}$ cfu/mL in untreated samples. The juice samples were subjected to thermal treatment at temperatures of 55, 65, 75, 85, and 95 °C for 0–12 min (Fig. 3a). The residual population of aerobic mesophiles was found to be 2.95, 2.12, and 1.45 $\log_{10}$ cfu/mL at 55, 65, and 75 °C, respectively, following a 12-min treatment. Conversely, at 85 and 95 °C for the same duration, the residual aerobic mesophiles population was determined to be below the detectable limit. Furthermore, the residual population of yeasts and molds
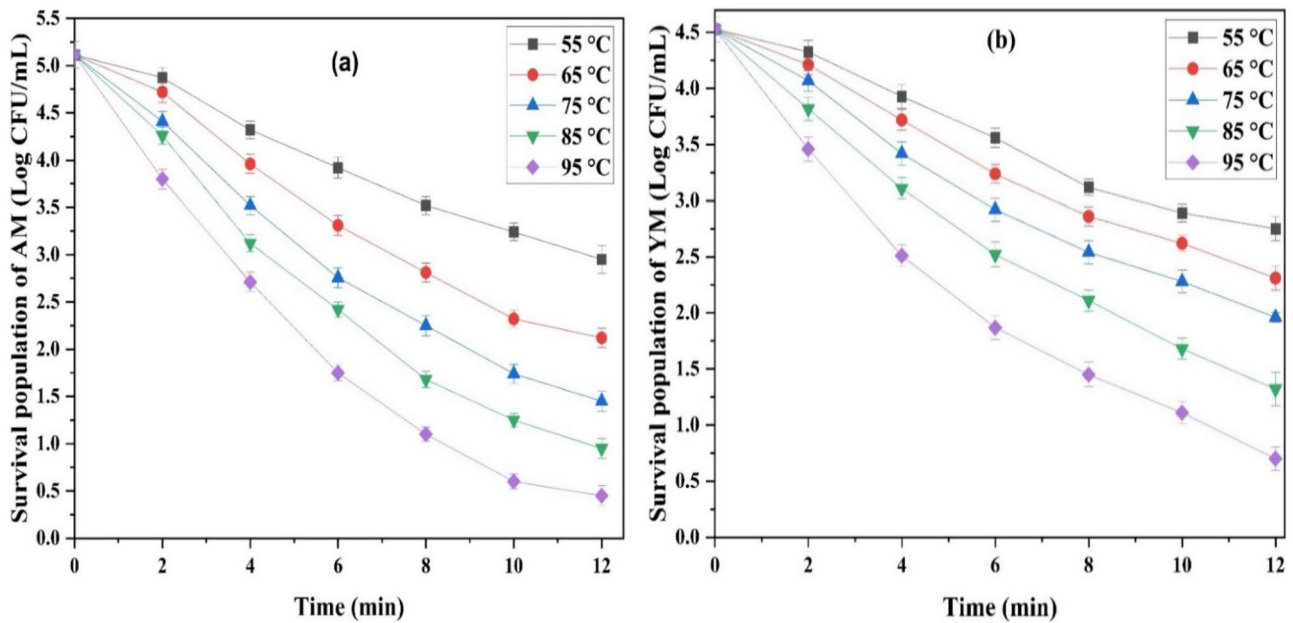
Fig. 3 Change in survival population with respect to time at various temperatures; **a** aerobic mesophiles (AM) and **b** yeasts and molds (YM)

was found to be 2.75, 2.31, 1.96, and 1.32 $\log_{10}$ cfu/mL at 55, 65, 75, and 85 °C respectively, following a 12-min treatment (Fig. 3b). However, at 95 °C for the same duration, the residual aerobic mesophiles population was determined to be below the detectable limit. Based on goodness of fit indicators ($R^2 = 0.90$–0.98 and RMSE = 0.74–5.49), the experimental data were well fitted to the 1st-order model for AM and YM, as shown in Table 1. The 1st kinetic model parameters showed that increasing the treatment temperature from 55 to 95 °C resulted in an inactivation rate (k) value increase of 0.43 to 1.06 min^{-1} for AM and 0.37 to 0.83 min^{-1} for YM (Table 1). The abovementioned finding showed that the inactivation of AM and YM increases with the increase in temperature. Elevated temperatures can harm the genetic material of microorganisms. DNA strands might fracture or undergo mutations, impeding microbial reproduction (Smelt & Brul, 2014). Heat induces greater instability in the lipids and proteins of microbial cell membranes (Cebrián et al., 2017). This heightened instability can cause cell membranes to disintegrate, causing the release of cell contents and eventual destruction of the cell.

Effect on PPO and POD Activity

Figure 4 illustrates the changes in enzyme activity for PPO and POD in PJ across different temperatures and treatment durations. The PPO residual activity reduced from 100 to 72% at 55 °C, 100 to 58% at 65 °C, 100 to 46% at 75 °C, 100 to 23% at 85 °C, and 100 to 4% at 95 °C for 0–12 min of thermal treatment (Fig. 4a). Based on goodness of fit

indicators ($R^2 = 0.98$–0.99 and RMSE = 0.15–1.25), the experimental data were well fitted to the Weibull model for PPO and POD, as shown in Table 1. The scale factor (δ) represents the time required to reduce enzyme activity by a factor of one logarithmic cycle (Pipliya et al., 2022). As the temperature increased from 55 to 95 °C, the δ value for PPO decreased from 36.51 to 4.76 min, as indicated in Table 1. These values of δ are negatively correlated with the treatment temperature regarding enzyme activity in PJ. This observation suggests that reducing the scale factor and elevating the treatment temperature would lead to heightened enzyme inactivation. Moreover, the PPO shape factors (β) ranged from 0.79 to 0.99, showing a concave upward inactivation curve for the Weibull distribution (Table 1). During thermal treatment, the application of high temperatures induces a distortion in the native conformation of PPO enzymes' protein structure. This distortion process disturbs the integrity of the enzyme's active sites, ultimately rendering them non-functional (Murtaza et al., 2018). Furthermore, the optimal function of PPO enzymes often hinges on the presence of specific cofactors, such as copper ions. The elevated temperatures encountered during thermal treatment can disrupt the stability of these essential cofactors, leading to the deactivation of the enzyme. Additionally, the interaction between the enzyme and its substrate molecules can be altered by heat. Consequently, inactivation can arise from shifts in the binding affinity or the accessibility of the substrate to the enzyme's active site.

Furthermore, the POD residual activity diminished from 100 to 76% at 55 °C, 100 to 62% at 65 °C, 100 to 49% at 75

Table 1 Kinetic model parameters and performance indicator for thermal treatment of pineapple juice at various temperatures

1st order kinetic model for AM and YM inactivation $(N = N_0 * e^{-k*t})$

	AM					YM				
Model parameters and performance indicator	55 °C	65 °C	75 °C	85 °C	95 °C	55 °C	65 °C	75 °C	85 °C	95 °C
k (min^{-1})	0.43±0.01[a]	0.62±0.01[b]	0.77±0.02[c]	0.91±0.03[d]	1.06±0.05[e]	0.37±0.01[a]	0.44±0.01[b]	0.50±0.01[b]	0.68±0.02[c]	0.83±0.05[d]
Adj. R^2	0.98	0.97	0.96	0.94	0.91	0.97	0.98	0.97	0.97	0.90
RMSE	0.74	1.55	2.33	3.66	5.49	1.02	1.02	1.84	1.76	4.05

2. Weibull kinetic model for PPO and POD inactivation $\left(A_t = A_o * e^{-(t/\delta)^\beta}\right)$

	PPO					POD				
Model parameters and performance indicator	55 °C	65 °C	75 °C	85 °C	95 °C	55 °C	65 °C	75 °C	85 °C	95 °C
δ (min)	36.51±1.55[e]	23.26±0.53[d]	16.45±0.16[c]	7.60±0.04[b]	4.76±0.16[a]	37.41±4.56[d]	24.23±0.86[c]	16.56±0.42[b]	8.83±0.12[a]	6.12±0.13[a]
β	0.99±0.02[d]	0.89±0.01[bc]	0.79±0.01[a]	0.84±0.01[ab]	0.94±0.06[cd]	1.12±0.10[b]	1.01±0.03[a]	1.03±0.05[a]	1.10±0.03[b]	1.07±0.06[a]
Adj. R^2	0.99	0.99	0.99	0.99	0.98	0.99	0.99	0.99	0.99	0.98
RMSE	0.20	0.22	0.15	0.22	1.25	0.54	0.33	0.43	0.58	1.05

Alphabets in lowercase (a, b, c, d, and e) in the superscripts denote that the mean values are statistically different within the row at p < 0.05

AM aerobic mesophiles, *YM* yeasts and molds, *PPO* polyphenol oxidase, *POD* peroxidase, *k* inactivation rate, *δ* scale parameter, *β* shape parameter, *Adj. R²* Adjusted coefficient of determination, *RMSE* root mean square error
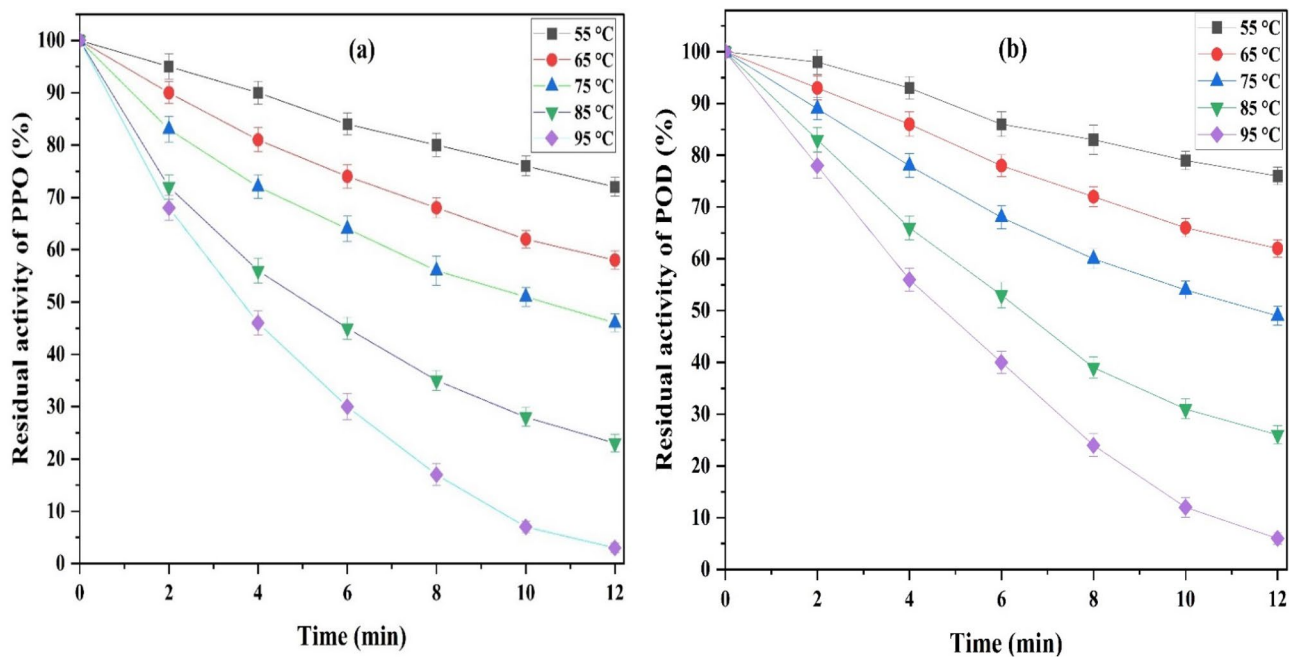
Fig. 4 Change in residual activity with respect to time at various temperatures; **a** polyphenol oxidase (PPO) and **b** peroxidase (POD)

°C, 100 to 26% at 85 °C, and 100 to 6% at 95 °C for 0–12 min of thermal treatment (Fig. 4b). Similar to PPO, elevated temperatures induce denaturation in POD enzymes. Similar to PPO, as the temperature increased from 55 to 95 °C, the δ value for POD decreased from 37.41 to 6.12 min (Table 1). Furthermore, the PPO shape factors (β) ranged from 1.01 to 1.12, indicating a convex downward pattern in the inactivation curve according to the Weibull distribution, as shown in Table 1. This denaturation disturbs the enzyme's tertiary and quaternary structures, impeding its catalytic activity. POD enzymes, akin to PPO, rely on cofactors such as hems groups or iron ions for their proper functioning. The application of thermal treatment can induce instability in these cofactors, resulting in a reduction of enzyme activity (Ercan & Soysal, 2011). Furthermore, heat can potentially modify the binding affinity and alignment of the enzyme's active site with its substrate. PPO and POD were inactivated more quickly at higher temperatures, as anticipated. The PPO and POD inactivation in PJ was shown to be influenced synergistically by thermal treatment factors, including temperature and the duration of treatment. The thermal treatment significantly ($p < 0.05$) reduced the activity of both enzymes.

Based on above-mentioned findings, the thermal treatment at 95 °C/12 min effectively reduced the residual activity of PPO and POD below 10% and the AMC and YMC beyond the detection limit. Therefore, the thermal treatment at 95 °C/12 min has been selected for further analysis.

Comparative Analysis of Untreated (S1), Optimized NTP–Treated (S2), extremely NTP–Treated (S3), and Thermally Treated (S4) Pineapple Juice

For the comparative analysis of PJ, untreated (S1), optimized NTP treated (38 kV/631 s, S2), extremely NTP treated (45 kV/900 s, S3), and thermally treated (95 °C/12 min, S4) have been taken for further study.

Comparison of Physicochemical, Nutritional, Phytochemical, and Enzymatic Quality Characteristics of Pineapple Juice During Various NTP and Thermal Treatments

The physicochemical characteristics, viz. pH, TA, and TSS content, exhibited insignificant ($p > 0.05$) variation across all samples (S1, S2, S3, and S4) (Table 2). This observation underscores the notion that applied voltage does not induce bond breakage, thus avoiding alterations in the concentration of H$^+$ ions within the medium. Similar findings were also reported in grape, orange, Sapota-do-Solimões juice, and apple juice after NTP treatment (Liao et al., 2018; Pankaj et al., 2017; Silva et al., 2022; Xu et al., 2017).

The color measurements revealed that elevating the NTP voltage led to a notable increase in browning within the sample. Specifically, the lightness and yellowness values decreased, while the redness values demonstrated an increase in correlation with the rise in NTP voltage

Table 2 Changes in quality attributes of pineapple juice during different CP and thermal treatments

Quality attributes	S1	S2	S3	S4
Color				
L*	34.34±0.67[a]	31.41±0.47[a]	26.16±0.31[b]	21.62±0.35[c]
a*	−2.42±0.11[a]	−0.36±0.05[b]	−0.58±0.03[c]	−0.47±0.05[d]
b*	8.04±0.77[a]	7.04±0.61[b]	5.26±0.43[c]	4.84±0.42[d]
ΔE*	-	2.13±0.23[a]	4.55±0.59[b]	8.12±0.45[c]
Physicochemical attributes				
pH	3.42±0.04[a]	3.40±0.02[a]	3.44±0.03[a]	3.45±0.02[a]
TSS	10.42±0.34[a]	10.55±0.41[a]	10.71±0.45[a]	10.83±0.31[a]
TA	5.02±0.33[a]	5.09±0.36[a]	4.98±0.34[a]	5.05±0.29[a]
Natural microflora (log$_{10}$ CFU/mL)				
AM	5.12±0.31	ND	ND	ND
YM	4.53±0.27	ND	ND	ND
Bioactive compounds				
AA	43.6±1.84[a]	39.24±1.51[b]	36.58±1.65[b]	13.08±1.10[c]
TPC	37.12±1.74[a]	37.4±1.52[a]	31.62±1.15[b]	11.45±0.61[c]
TFC	7.52±0.43[a]	7.35±0.31[a]	6.31±0.36[b]	1.89±0.14[c]
TAC	14.4±1.42[a]	14.18±1.10[a]	11.54±0.89[b]	4.75±0.65[c]
Relative enzyme activity (%)				
PPO	100	6.58±1.31[a]	3.15±0.8[b]	2.94±0.9[b]
POD	100	9.89±1.42[a]	2.31±1.4[b]	2.45±0.72[b]
BRM	100	51.3±2.57[a]	33.6±1.57[b]	10.70±1.3[c]

Alphabets in lowercase (a, b, c, and d) in the superscripts denote that the mean values are statistically different within the row at $p < 0.05$

TSS total soluble solid, *TA* titratable acidity, *AM* aerobic mesophiles, *YM* yeasts and molds, *AA* ascorbic acid, *TPC* total phenolic content, *TFC* total flavonoid content, *TAC* total antioxidant capacity, *PPO* polyphenol oxidase, *POD* peroxidase, *BRM* bromelain, *S1* untreated, *S2* optimized plasma treated (38 kV/631 s), *S3* extremely plasma treated (45 kV/900 s), *S4* thermally treated (95 °C/12 min)

(Table 2). However, in S2 samples, the ΔE* was acceptable after NTP treatment (Kumar et al., 2023a). Concerning samples S3 and S4, the reduced probabilities of enzymatic browning were indicated by 4% and 3% residual PPO activities, respectively. However, the corresponding ΔE* values of 6.9 and 9.5 were deemed unacceptable. The higher ΔE* observed in S3 and S4, compared to S2, could be attributed to pigment degradation by reactive plasma species and the acceleration of non-enzymatic browning, particularly at elevated temperatures. The observed alteration in color of the extremely NTP–treated sample can be attributed to the isomerization of coloring compounds (pigments) and the oxidation processes caused by reactive species that are formed as a result of the NTP treatment (Onal-Ulusoy, 2021; Sruthi et al., 2022).

In the S1, the aerobic mesophiles microbial population was found to be 5.12 log$_{10}$ cfu/mL, while the count for yeasts and molds stood at 4.53 log$_{10}$ cfu/mL (Table 2). Employing the optimized condition of 38 kV/631 s (S2) effectively reduced the microbial counts of both natural microbiota groups to levels below detection thresholds. Similar reduction of aerobic mesophile and yeasts and molds was also

reported on strawberry surface (Misra et al., 2014) and saffron (Khodabandeh et al., 2023) after plasma treatment. In addition, Khodabandeh et al. (2023) also showed the reduction of coliforms and *E. coli* in plasma-treated (power: 76 W and treatment time: 26 min) saffron by 6.71 and 6.07 log cfu/g, respectively (Khodabandeh et al., 2023). The microbial inactivation of NTP may be attributed to the deadly effects of ions and highly reactive species, such as reactive oxygen species (ROS) and reactive nitrogen species (RNS), which interact with the cellular biological components (Mol et al., 2023; Mousavi et al., 2022). In addition, the antimicrobial effect may be augmented by the presence of various atoms, metastable compounds, and radicals, as well as short-lived and long-lived neutral reactive species (Wang et al., 2016; Xu et al., 2020). Additionally, the samples S3 and S4 also demonstrated microbial populations below the detection limit. Pipliya et al. (2023a) also revealed the survival population of AM and YM in pineapple was obtained below the detection limit after NTP treatment at 35 kV for 10 min. Chakraborty et al. (2015b) also reported the AM and YM in pineapple puree below the detection limit after thermal treatment (95 °C/12 min).

The TPC in samples S1 and S2 displayed statistical similarity, indicating the stability of phenolics under optimized conditions (Table 2). Compared to S1, a minor increase in phenolic content in S2 could be attributed to enhanced extractability facilitated by the action of reactive oxygen and nitrogen species on the juice samples. Similar observation was observed during the plasma treatment of Sapota-do-Solimões juice (Silva et al., 2022), white *C. militaris* (Sangwanna et al., 2023), chokeberry (Gan et al., 2021), and caja juice (Rodriguez et al., 2022). In the case of sample S3, there was a notable 14% reduction in phenolic content. This finding was attributable to the prolonged exposure of juice samples to NTP treatment at the higher applied voltage resulted in the degradation of phenolic components. This degradation was induced by the oxidation of polyphenols by reactive oxygen species and free radicals (Kumar et al., 2023a). These phenolic compounds are susceptible to thermal treatment. Therefore, treatment at 95 ℃ for 12 min led to 70% degradation of phenolic compounds in sample S4. The relative antioxidant activities were 98.7%, 81%, and 33% for samples S2, S3, and S4, respectively (Table 2). AA is highly susceptible to ultraviolet (UV) radiation, reactive oxygen species (ROS), and ozone. Therefore, AA losses in samples S2, S3, and S4 were 10%, 16%, and 71%, respectively (Table 2). AA oxidation occurred due to its interaction with NTP-generated species, leading to its degradation after the NTP exposure. AA serves as an agent that eliminates free radicals, namely those formed in NTP. These free radicals are responsible for inducing instability in the AA present in the juice, leading to modifications in the original properties of its constituents (Tiwari et al., 2008). The decrease in TAC in S3 and S4 could be attributed to the reactive species and thermal sensitivity of these compounds due to their radical nature.

Comparatively, NTP treatment led to a lesser degree of enzyme inactivation than the thermal treatment. For S3 and S4, the inactivation rates of PPO were notably high at 96% and 97%, respectively, while sample S2 exhibited a 93% reduction (Table 2). The residual activity of polyphenol oxidase (PPO) and peroxidase (POD) in banana and mushroom samples was observed to be less than 10% following NTP treatment (Khoshkalam Pour et al., 2022; Surowsky et al., 2013). This phenomenon contributed to the stabilization of juice and extended its shelf life during storage. The observed inactivation of PPO and POD in the NTP-treated samples can be attributed to the disruption of secondary structure, namely the loss of β-sheet and α-helix conformations, as well as the denaturation of enzyme in PJ. These changes are likely caused by the interaction of charged NTP species with PPO and POD enzymes (Kumar et al., 2023c; Pipliya et al., 2022). Regarding BRM activity, the retention percentages were 51% for S2, 37% for S3, and 11% for S4 (Table 2). As previously discussed, in samples S2 and S3, the correlation between voltage and time synergistically contributed to PPO inactivation, with voltage playing a major role. The activity of bromelain showed a reduction as a result of the presence of robust electrostatic forces and reactive species generated during NTP treatment. These factors can potentially induce the unfolding and denaturation of the structure of the enzyme.

Evidently, the product treated with optimized NTP (S2) exhibited superiority over S3 and S4 concerning the retention of bromelain, bioactive compounds, physicochemical, and nutritional quality attributes. Importantly, optimized NTP effectively prevented any microbial risks associated with the product. In contrast, the thermally treated sample (S4) experienced a significant loss of beneficial pineapple bioactive compounds and underwent similar microbial reduction, despite a higher degree of enzyme inactivation than the NTP process. Nonetheless, samples S3 and S4 demonstrated stability compared to S2 regarding residual PPO and POD activity. Lower enzyme inactivation may have an

Table 3 Similarity values and ranking for the samples and quality attributes based on the sensory evaluation

Scale factor	Sample				Quality attributes				
	S1	S2	S3	S4	Color	Aroma	Taste	Mouthfeel	Aftertaste
Not satisfactory, F1	0.000	0.000	0.031	0.216	0.000	0.000	0.000	0.000	0.000
Fair, F2	0.042	0.065	0.296	0.768	0.000	0.000	0.000	0.000	0.000
Satisfactory, F3	0.261	0.314	0.678	**0.778**	0.033	0.080	0.064	0.064	0.120
Good, F4	0.566	0.620	**0.692**	0.248	0.489	0.680	0.618	0.618	0.746
Very good, F5	**0.733**	**0.714**	0.295	0.008	**0.981**	**0.871**	**0.894**	**0.858**	**0.813**
Excellent, F6	0.323	0.279	0.027	0.000	0.367	0.210	0.240	0.186	0.128
Ranking	I	II	III	IV	I	III	II	IV	V

The bold numbers are shown the maximum similarity values corresponding to each column

S1 untreated pineapple juice, *S2* optimized plasma treated, *S3* Extremely plasma treated, *S4* conventional thermal treatment, *F1* not at all necessary, *F2* somewhat necessary, *F3* necessary, *F4* important, *F5* highly important, *F6* extremely important

impact on the storage durability of NTP-treated sample (S2), but their significantly higher nutritional quality compared to thermally treated (S4) may make up for it.

Fuzzy Logic Sensory Evaluation

The sensory score and triplet for the sensory score associated with each attribute are displayed in Table S2. The majority of sensory panelists assigned ratings of "very good" or "excellent" to all quality attributes for the untreated sample, as shown in Table S2. For the majority of sensory quality characteristics, a greater number of panelists assigned higher scores to the optimized NTP sample (S2) in comparison to S3 and S4, as indicated in Table S2. The ranking attributed to various quality attributes of PJ, in general, ranging from the "important" to "extremely important" categories for the purpose of sample characterization.

The triplet scores assigned to all the samples exhibited a clear trend of superiority, with the order being S1 > S2 > S3 > S4 in terms of most sensory quality characteristics. This trend highlights that extremely NTP–treated and thermally treated juice reduced product acceptability among the panelists. According to the standard 6-point sensory scale (fuzzy scale), samples S1 and S2 were classified within the "good" category, while S3 and S4 fell into the "satisfactory" and "fair" groups, respectively. Similar to physicochemical quality characteristics, the optimized NTP sample (S2) closely resembles the sensory characteristics of the untreated sample (S1) as both samples exhibit a significantly high level of importance, with similarity values of 0.73 and 0.70 for S1 and S2, respectively. The alteration in color and the reduction in other bioactive components are the least in S2 compared to the untreated sample (S1). Consequently, it is evident that the importance given to S1 and S2 are similar (very good), and the similarity values for S1 and S2 are close to each other. The loss of bioactive substances in S4 is comparatively higher than in S3, as indicated by their rankings in Table 3.

The overall rating of the sensory quality characteristics of PJ in general indicates that all of the sensory qualities are deemed to be "highly important" for the acceptability of the product (Table 3). When comparing the sensory quality aspects in terms of similarity scores for PJ, color is identified as the leading contributor (0.98), followed by taste (0.89), aroma (0.87), mouthfeel (0.85), and aftertaste (0.81). Fruit juice tends to be very popular due to its distinctive flavor and taste, which draws consumers' attention. Additionally, color is one of the most essential characteristics of fruit juice's acceptability among consumers (Chakraborty et al., 2015a). The rating of the quality qualities determined during the sensory evaluation of the PJ reflects both of these facts.

The similarity values for quality attributes of PJ for all four samples are shown in Table 4. The sensory quality attributes of the S1 and S2 received importance ranging from "excellent" to "very good," while the S3 and S4 were ranked from "good" to "fair." The ranking of the sensory characteristics of all 4 samples indicates that the S1 and S2 samples are preferred over S3 and S4 samples by the panelists for consumption. Based on similarity values of sample S2, mouthfeel (0.88) is the most preferred attribute by panelists, followed by taste (0.79), aroma (0.74), aftertaste

Table 4 Similarity values for quality attributes of pineapple juice for individual sample

Scale factor	Quality attributes				
	Color	Aroma	Taste	Mouthfeel	Aftertaste
S1					
Not satisfactory, F1	0.003	0.000	0.000	0.000	0.000
Fair, F2	0.104	0.019	0.000	0.013	0.021
Satisfactory, F3	0.355	0.203	0.020	0.183	0.208
Good, F4	0.611	0.517	0.206	0.525	0.514
Very good, F5	**0.643**	**0.835**	0.522	**0.885**	**0.817**
Excellent, F6	0.254	0.506	0.710	0.554	0.487
S2					
Not satisfactory, F1	0.005	0.000	0.000	0.000	0.000
Fair, F2	0.117	0.040	0.000	0.013	0.048
Satisfactory, F3	0.372	0.235	0.038	0.183	0.250
Good, F4	**0.624**	0.501	0.268	0.525	0.515
Very good, F5	0.622	**0.741**	0.599	**0.885**	**0.734**
Excellent, F6	0.232	0.413	**0.793**	0.554	0.393
S3					
Not satisfactory, F1	0.039	0.027	0.000	0.000	0.127
Fair, F2	0.267	0.230	0.063	0.064	0.511
Satisfactory, F3	0.578	0.527	0.279	0.277	**0.755**
Good, F4	**0.679**	**0.669**	0.543	0.531	0.511
Very good, F5	0.411	0.456	**0.707**	**0.711**	0.138
Excellent, F6	0.099	0.131	0.336	0.355	0.000
S4					
Not satisfactory, F1	0.243	0.191	0.090	0.115	0.163
Fair, F2	**0.730**	0.660	0.376	0.495	0.619
Satisfactory, F3	0.764	**0.741**	**0.663**	**0.753**	**0.784**
Good, F4	0.270	0.398	0.617	0.520	0.439
Very good, F5	0.016	0.058	0.286	0.153	0.086
Excellent, F6	0.000	0.000	0.040	0.004	0.000

The bold numbers are shown the maximum similarity values corresponding to each column for each sample

S1 untreated pineapple juice, *S2* optimized plasma treated, *S3* Extremely plasma treated, *S4* Conventional thermal treatment, *F1* not at all necessary, *F2* somewhat necessary, *F3* necessary, *F4* important, *F5* highly important, *F6* extremely important

(0.73), and color (0.62), as shown in Table 4. The better mouthfeel of S2 samples might be attributable to the reduced particle size that provides better consistency. For sample S3, the aftertaste (0.75) has the highest similarity value, followed by mouthfeel (0.71), taste (0.70), color (0.67), and aroma (0.66). The lowest similarity value of aroma/flavor of the extremely NTP–treated sample (S3) may be due to the oxidation of the flavonoid compound, which degraded the flavor of the sample. Eventually, the similarity values for the thermally treated sample (S4) for sensory attributes ranked as an aftertaste, mouthfeel, aroma, color, and taste. For the thermally treated sample (S4), aftertaste (0.79) is the most preferred attribute by panelists, followed by color (0.78), mouthfeel (0.75), aroma (0.74), and taste (0.66) based on similarity values (Table 4). A thermally treated juice sample (S4) developed a cooked flavor as a result of the thermal treatment. Therefore, the panelists gave the lowest similarity value of the aroma for the S4 sample. Moreover, the lowest importance of color (Fair) in sample S4 indicated that the thermal treatment was responsible for the non-enzymatic browning and pigment degradation of the juice sample (Landl et al., 2010).

Based on fuzzy logic sensory evaluation findings, the optimized NTP–treated sample (S2) had similar sensory quality characteristics to the untreated sample (S1). In contrast, the sensory qualities of the NTP-treated (S3) and thermally treated (S4) samples were diminished compared to the untreated (S1) and optimized treated (S2) samples.

Particle Size Distribution

The impact of NTP and thermal treatment on the particle size is shown in Table 5 and Fig. 5. The particle size is decreased by the application of NTP and thermal treatment, which increases the stability of PJ. The PJ samples (S1, S2, S3, and S4) exhibited varying mean diameters. The obtained volume mean diameters ($D_{(4, 3)}$) were 1688.37 nm, 1100.18 nm, 917.96 nm, and 1065.23 nm for S1, S2, S3, and S4, respectively. Meanwhile, the sauter mean diameters

($D_{(3, 2)}$) were 1617.63 nm, 1048.85 nm, 894.52 nm, and 1005.7 nm for S1, S2, S3, and S4, respectively. Notably, the $D_{(4, 3)}$ values were consistently higher than the corresponding $D_{(3, 2)}$ values across all samples. This discrepancy suggests the prevalence of larger particles in the juices compared to smaller particles. This observation remains consistent for NTP and thermally treated juices. In comparison to the untreated sample (S1), the optimized NTP (S2), extremely NTP (S3), and thermally treated (S4) juice samples exhibited considerably ($p < 0.05$) lowered $D_{(4, 3)}$, $D_{(3, 2)}$, $D_{(v, 0.90)}$, $D_{(v, 0.50)}$, and $D_{(v, 0.10)}$ PSD values (Table 5). The NTP processing resulted in a considerable reduction in the size of the suspended particles, which stabilized the juice. Wang et al. (2022) also revealed that augmenting the applied voltages during NTP treatment resulted in a substantial reduction in the particle size of jujube juice. According to Illera et al. (2019), homogenization occurs when the particle size decreases, improving the stability of fruit juice. PJ that had been thermally and NTP processed both had a monomodal distribution (Fig. 5). The PSD span value was much lower in the NTP-treated samples (S2 and S3) than in the thermally treated samples (S4). The particle distribution width of PJ is defined by its span value. Therefore, a decrease in span value indicates more homogenization of the juice (higher uniformity of particles in lower span) that finally results in the stabilization of the juice.

Effect on Rheological Characteristics

Rheology is the science that deals with fluids' deformation and flow behavior. When it comes to food, understanding its rheological properties holds significant importance for tasks such as designing operational units, optimizing processes, and ensuring superior-quality products. Consequently, investigating how processing impacts the rheological characteristics of food is of paramount importance in creating efficient product designs and techniques (Augusto et al., 2012). In this regard, an examination was conducted on the rheological attributes (including shear stress, apparent viscosity,

Table 5 Effect of different non-thermal plasma and thermal treatments on the particle size of pineapple juice

Particle size	Sample			
	S1	S2	S3	S4
$D_{(3, 2)}$	1617.63 ± 33.12^d	1048.85 ± 31.26^c	894.52 ± 28.42^a	$1005.71 \pm 34.26b$
$D_{(4, 3)}$	1688.37 ± 42.23^d	1100.18 ± 27.53^c	$917.96 \pm 34.42a$	1065.23 ± 24.23^b
$D_{(v, 0.9)}$	1800.22 ± 45.41^d	1160.18 ± 34.45^c	979.09 ± 25.12^a	1120.15 ± 35.76^b
$D_{(v, 0.5)}$	1341.48 ± 31.56^c	910.25 ± 23.56^b	777.20 ± 28.25^a	786.54 ± 29.23^a
$D_{(v, 0.1)}$	993.57 ± 26.13^c	649.84 ± 26.42^{bc}	617.65 ± 29.35^b	507.71 ± 24.21^a
Span	0.60 ± 0.02^c	0.56 ± 0.02^b	0.46 ± 0.03^a	0.77 ± 0.04^d

Alphabets in lowercase (a, b, c, and d) in the superscripts denote that the mean values are statistically different within the row at p < 0.05

$D_{(3, 2)}$ sauter mean diameter, $D_{(4, 3)}$ volume mean diameter, *S1* untreated pineapple juice, *S2* optimized plasma treated, *S3* extremely plasma treated, *S4* conventional thermal treatment

Fig. 5 Particle size of pineapple juice: S1, untreated; S2, optimized NTP treated; S3, extremely NTP treated; S4, thermally treated pineapple juice
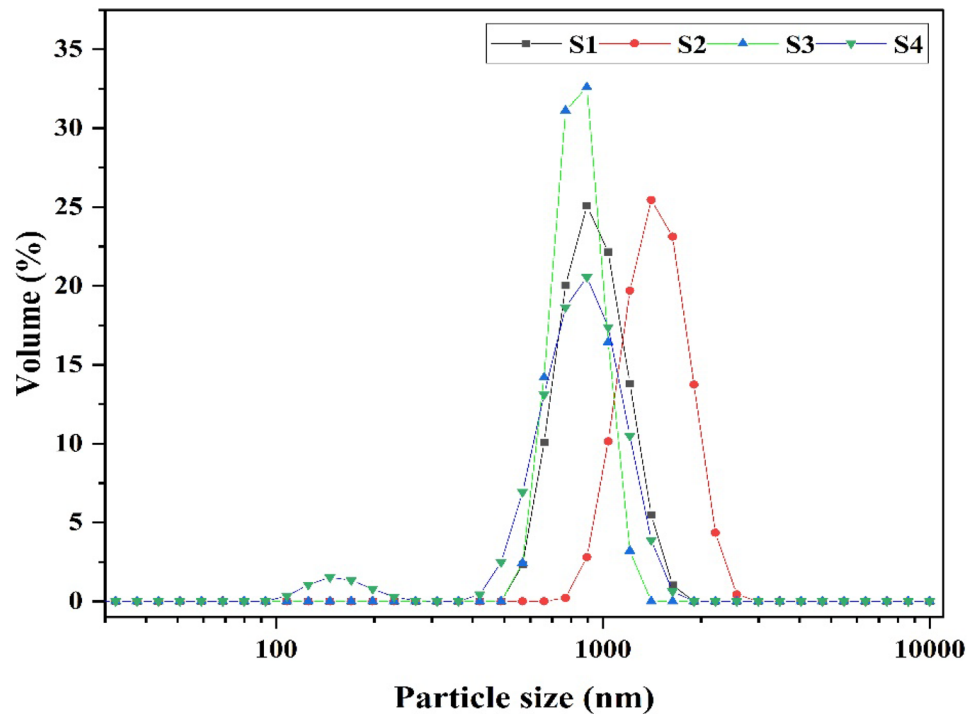
storage modulus, and loss modulus) of untreated thermally and optimized NTP-treated PJ.

Flow Response of Pineapple Juice

A range of factors influences the selection of an appropriate rheological model to characterize distinct fluid behaviors. Different models have been employed to delineate the flow characteristics of fluids, whether they conform to Newtonian ($n = 1$) or non-Newtonian ($n \neq 1$) behaviors. Various rheological characteristics encompass n (flow behavior index), τ_o (yield stress), K (consistency index), and R^2 (coefficient of determination) according to the Herschel–Bulkley model. The untreated (S1), optimized NTP–treated (S2), extremely NTP–treated (S3), and thermally treated (S4) juice samples exhibited non-Newtonian pseudo-plastic behavior ($n < 1$). K

Table 6 Effect of thermal and CP treatment on rheological properties fitted to the Herschel–Bulkley model

Treatments	K (mPa.s^n)	n	τ_o (mPa)	R^2
S1	1.22 ± 0.14^c	0.31 ± 0.06^b	0.33 ± 0.03^a	0.99
S2	0.68 ± 0.06^b	0.41 ± 0.01^c	0.58 ± 0.07^b	0.99
S3	0.31 ± 0.05^a	0.55 ± 0.02^d	0.73 ± 0.05^c	0.99
S4	0.34 ± 0.02^a	0.15 ± 0.02^a	1.07 ± 0.07^d	0.99

Alphabets in lowercase (a, b, c, and d) in the superscripts denote that the mean values are statistically different within the column at p < 0.05

K consistency index, n flow behavior index, τ_o yield stress, R^2 coefficient of determination, *S1* untreated pineapple juice, *S2* optimized plasma treated, *S3* extremely plasma treated, *S4* conventional thermal treatment

of all samples varied significantly ($p < 0.05$) after thermal and NTP treatment. The results indicate that NTP processing decreased K compared to untreated samples (Table 6). Manzoor et al. (2023) also reported a similar finding on the use of the dielectric barrier discharge plasma technology for treating wheat sprout juice. The reduction in apparent viscosity as the shear rate increases signifies rapid initial shearing breakdown (Fig. 6b). On the contrary, noticeable structural changes occur at high shear rates. These findings align with the results from the PSD analysis, where NTP treatment disrupted aggregates and generated smaller structures of juice particles. These alterations reduced consistency and non-Newtonian ($n \neq 1$) fluid characteristics (Table 6). The diminished particle size enhances dispersibility and fills the gaps between larger particles, resulting in a lubricating effect that lowers apparent viscosity. Shear stress (mPa) was graphed against shear rate (s^{-1}) for untreated, thermally treated, and NTP-treated samples to elucidate the flow behavior (n) of PJ (Fig. 6a). In the context of NTP treatment, an increase in voltages resulted in a reduction of shear stress compared to untreated and thermally treated samples. Additionally, at high shear rates, the structure undergoes less alteration.

Dynamic Rheological Characteristics of Pineapple Juice

We examined the performance of the storage modulus (G′) and loss modulus (G″) across a frequency range of 0.1 to 10 Hz, as depicted in Fig. 6c and d. This evaluation was carried out using a frequency sweep approach. Relative
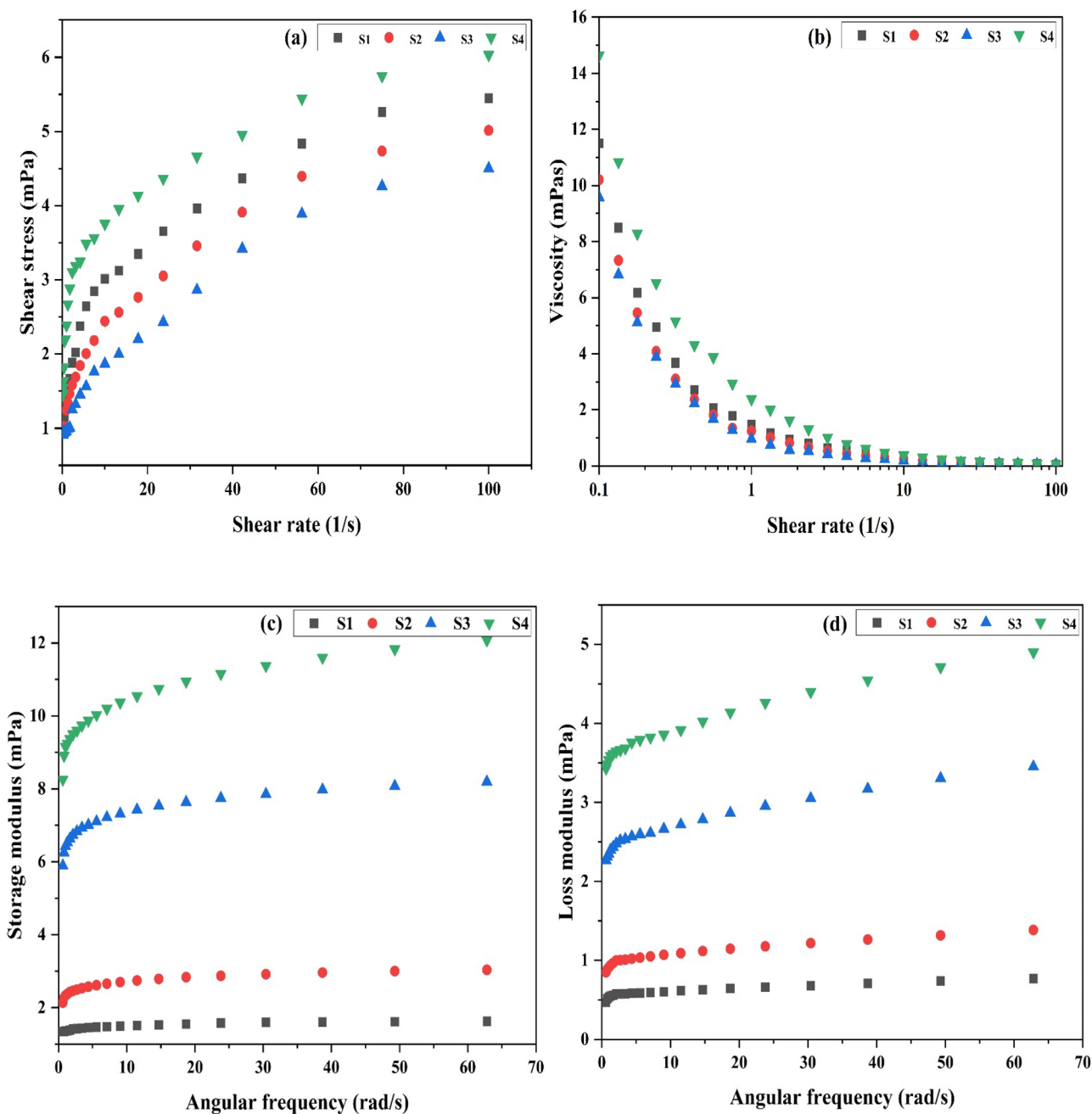
Fig. 6 Rheological properties of untreated (S1), optimized NTP treated (S2), extremely NTP treated (S3), and thermally treated (S4) pineapple juice: **a** shear stress; **b** apparent viscosity; **c** storage modulus; **d** loss modulus

to the untreated samples (S1), the PJ samples subjected to extreme NTP (S3) and thermal (S4) treatments exhibited an upward trend in the storage modulus (G′) and loss modulus (G″) values as the frequency increased except untreated (S1) and optimized NTP (S2) treated juice sample. Compared to untreated samples at the same frequency, an increase in G′ and G″ was observed in NTP and thermally treated PJ. Similar results were obtained when kiwifruit juice and mango nectar were exposed to higher-intensity ultrasonic treatment

(Huang et al., 2018; Wang et al., 2019). Moreover, the most pronounced G′ and G″ values were detected in the thermal treatment, succeeded by untreated and different NTP-treated samples. Nevertheless, the change in G′ and G″ between untreated and optimized NTP–treated juice samples was statistically insignificant. Additionally, the results showed that at a frequency between 0.1 and 10 Hz, the value of G′ is greater than G″, which is consistent with the outcomes of ultrasonic treatments of mango nectar and kiwifruit

juice (Huang et al., 2018; Wang et al., 2019). Moreover, the rheological attributes of fruit juices, along with complex alteration after NTP treatment, are heavily influenced by the variety of fruit used and the juice concentration (Suo et al., 2022b). Nevertheless, the existing researches on the impact of NTP treatment on the rheological characteristics of fruit juices are rare. Therefore, more investigations are necessary to validate the underlying mechanism of this transformation.

Effect on the Secondary Structure of a Protein

The infrared spectra of proteins often include the Amide-I region (1600–1700 cm^{-1}), which is particularly responsive to variations in their secondary structure, such as β-sheets, α-helix, random coils, anti-parallel β-sheet, and β-turns. Due to this sensitivity, we selected the Amide-I region to assess the relative proportions of distinct secondary structures within proteins present in untreated (S1), optimized NTP (S2), and thermally (S4) treated PJ (Fig. 7). Upon conducting FTIR spectral analysis of the protein samples from these sets, distinct Gaussian bands spanning the range of 1615 to 1692 cm^{-1} were observed within the Amide-I region. These bands correspond to various structural elements β-sheets, α-helix, random coils, anti-parallel β-sheet, and β-turns. After thermal treatment, there was a reduction in the presence of β-sheets and α-helix within the protein structure of the juice sample, compared to the untreated sample, as indicated in Table 7. The changes in β-sheets, α-helix, random coils, anti-parallel β-sheet, and β-turns might be attributable to the highly reactive (reactive oxygen and nitrogen species) species generated after plasma treatment. The presence of reactive species leads to the oxidative degradation
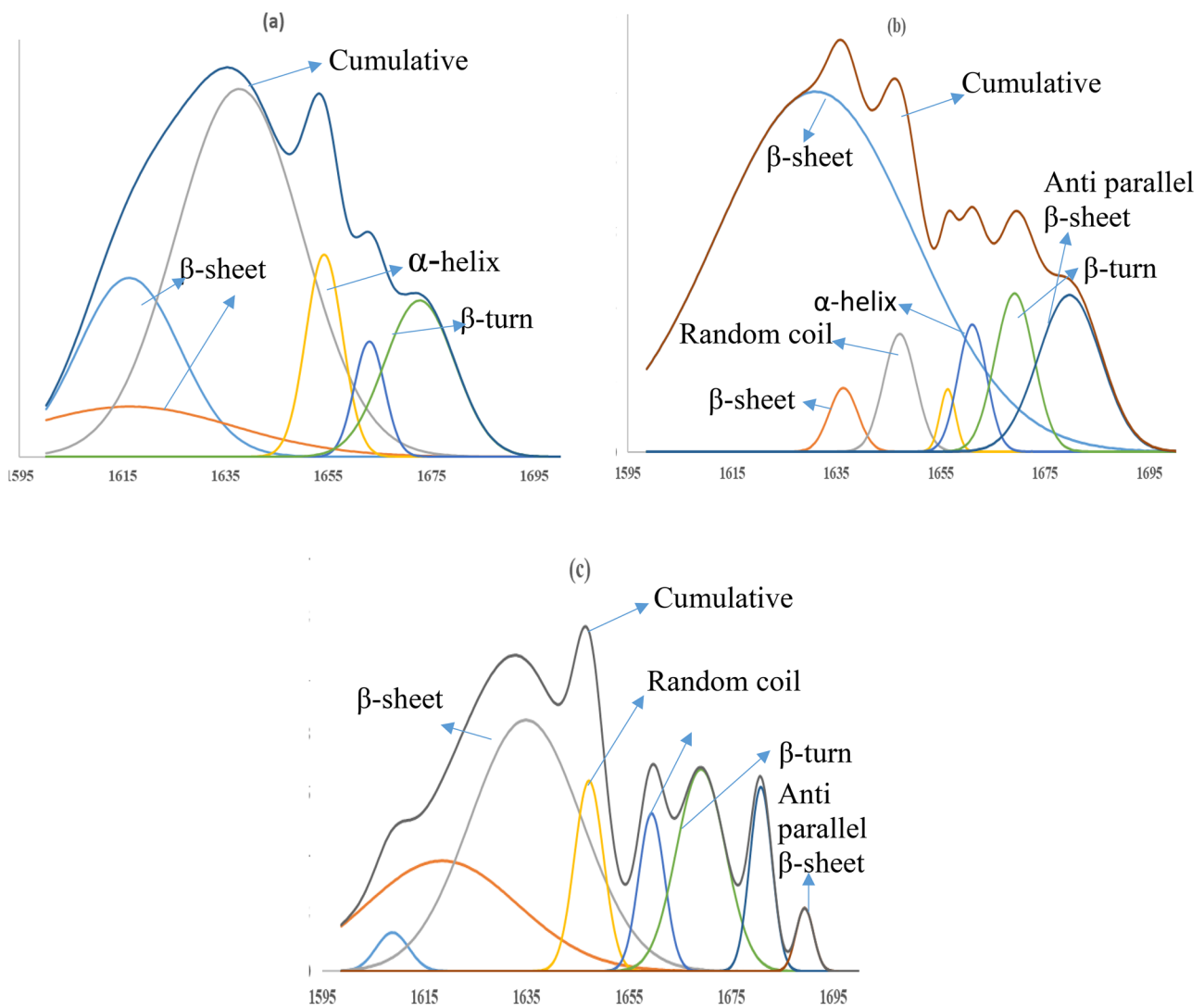

Fig. 7 Spectral deconvolution of the Amide-I band of pineapple juice protein: **a** untreated (S1); **b** optimized NTP (S2); **c** thermally treated (S4)

Table 7 Alteration in the secondary structure of the protein in pineapple juice after different treatment

Treatment	Secondary structure of the protein				
	β-sheet	α-helix	β-turn	Random coil	Anti-parallel β-sheet
S1	47.74	11.24	11.24	-	29.74
S2	74.95	4.75	6.29	3.90	10.09
S4	39.6	5.77	13.97	7.81	31.04

S1 untreated pineapple juice, *S2* optimized plasma treated, *S4* conventional thermal treatment

of proteins, resulting in the cleavage of peptide bonds, modification of amino acid residues, and fragmentation of polypeptide chains. These processes together contribute to the alteration of the protein's secondary structure (Pipliya et al., 2022).

Baltacioılu et al. (2015) also reported the loss of the α-helix and β-sheets structure of protein and PPO after thermal treatment. Conversely, the optimized NTP treatment (S2) exhibited an augmentation in β-sheets content and a reduction in the α-helix structure within the secondary protein structure of the juice sample compared to the untreated sample, as shown in Table 7. Segat et al. (2016) also reported a similar finding in alkaline phosphatase enzyme protein structure after NTP treatment. These findings suggested that the inactivation of PPO and POD after thermal and NTP treatments might be attributed to modifications in the secondary protein structure. These modifications encompass variations in the structure like elements β-sheets, α-helix, random coils, anti-parallel β-sheet, and β-turns.

Conclusion

To sum up, the impact of several NTP and thermal treatments on enzyme activity, microbial growth, protein structure, particle size, nutritional composition, sensory properties, phytochemical content, and rheological characteristics of PJ was investigated in this work. The product treated with optimized NTP (S2) exhibited superiority over S3 and S4 concerning the retention of bromelain, bioactive compounds, and physicochemical and nutritional quality attributes. Similar to thermal techniques, the NTP technique also guarantees an extension of shelf life by ensuring microbial safety and inducing effective enzyme inactivation. Furthermore, the use of the NTP technique resulted in a notable decrease in particle size, leading to a reduction in consistency index (K) and an indication of pseudo-plastic behavior ($n < 1$). Consequently, these alterations contributed to the enhanced stability of PJ. Fuzzy logic sensory evaluation showed that the optimized NTP–treated sample (S2) had comparable sensory

quality to the untreated sample (S1). The NTP-treated (S3) and thermally treated (S4) samples had lower sensory quality than the untreated (S1) and optimized treated (S2) samples. The NTP and thermal treatment are also responsible for altering protein secondary structure. Hence, NTP processing emerges as a promising novel technique for producing microbiologically safe and enzymatically stable PJ and maintaining its overall quality. In summary, it can be concluded that emerging technologies like NTP treatment can be efficiently employed on an industrial level to preserve and process PJ.

Supplementary Information.

Declarations

Ethical Approval Not applicable.

Competing Interests The authors declare no competing interests.

References

Alves Filho, E. G., Silva, L. M. A., de Brito, E. S., Castro, D. R. G., Bezerra, J. A., Sanches, E. A., Rodrigues, S., Fernandes, F. A. N., & Campelo, P. H. (2021). Effect of glow and dielectric barrier discharges plasma on volatile and non-volatile chemical profiling of camu-camu juice. *Food and Bioprocess Technology, 14*(7), 1275–1286. https://doi.org/10.1007/S11947-021-02639-6/TABLES/4

Ashtiani, S. H. M., Aghkhani, M. H., Feizy, J., & Martynenko, A. (2023). Effect of cold plasma pretreatment coupled with osmotic dehydration on drying kinetics and quality of mushroom (Agaricus bisporus). *Food and Bioprocess Technology, 1*, 1–23. https://doi.org/10.1007/S11947-023-03096-Z/TABLES/4

Augusto, P. E. D., Ibarz, A., & Cristianini, M. (2012). Effect of high pressure homogenization (HPH) on the rheological properties of a fruit juice serum model. *Journal of Food Engineering, 111*(2), 474–477. https://doi.org/10.1016/j.jfoodeng.2012.02.033

Baltacioglu, H., Bayindirli, A., Severcan, M., & Severcan, F. (2015). Effect of thermal treatment on secondary structure and conformational change of mushroom polyphenol oxidase (PPO) as food quality related enzyme: A FTIR study. *Food Chemistry, 187*, 263–269. https://doi.org/10.1016/j.foodchem.2015.04.097

Basak, S. (2018). The use of fuzzy logic to determine the concentration of betel leaf essential oil and its potency as a juice preservative. *Food Chemistry, 240*, 1113–1120. https://doi.org/10.1016/j.foodchem.2017.08.047

Cebrián, G., Condón, S., & Mañas, P. (2017). Physiology of the inactivation of vegetative bacteria by thermal treatments: Mode of action, influence of environmental factors and inactivation kinetics. *Foods, 6*(12), 1–21. https://doi.org/10.3390/foods6120107

Chakraborty, S., Rao, P. S., & Mishra, H. N. (2015a). Effect of combined high pressure-temperature treatments on color and nutritional quality attributes of pineapple (Ananas comosus L.) puree. *Innovative Food Science and Emerging Technologies, 28*, 10–21. https://doi.org/10.1016/j.ifset.2015.01.004

Chakraborty, S., Rao, P. S., & Mishra, H. N. (2015b). Response surface optimization of process parameters and fuzzy analysis of sensory data of high pressure–temperature treated pineapple puree. *Journal of Food Science, 80*(8), E1763–E1775. https://doi.org/10.1111/1750-3841.12967

Cheng, J. H., Wang, H., & Sun, D. W. (2023). Insight into the IgE-binding sites of allergenic peptides of tropomyosin in shrimp (Penaeus chinensis) induced by cold plasma active particles. *International Journal of Biological Macromolecules, 234*, 123690. https://doi.org/10.1016/J.IJBIOMAC.2023.123690

da Costa Pinto, C., Sanches, E. A., Clerici, M. T. P. S., Rodrigues, S., Fernandes, F. A. N., de Souza, S. M., Teixeira-Costa, B. E., de Araújo Bezerra, J., Lamarão, C. V., & Campelo, P. H. (2023). Modulation of the physicochemical properties of aria (Goeppertia allouia) starch by cold plasma: Effect of excitation frequency. *Food and Bioprocess Technology, 16*(4), 768–784. https://doi.org/10.1007/S11947-022-02970-6/TABLES/3

Ercan, S. Ş., & Soysal, Ç. (2011). Effect of ultrasound and temperature on tomato peroxidase. *Ultrasonics Sonochemistry, 18*(2), 689–695. https://doi.org/10.1016/j.ultsonch.2010.09.014

Feizollahi, E., & Roopesh, M. S. (2021). Degradation of zearalenone by atmospheric cold plasma: Effect of selected process and product factors. *Food and Bioprocess Technology, 14*(11), 2107–2119. https://doi.org/10.1007/S11947-021-02692-1/TABLES/5

Gan, Z., Feng, X., Hou, Y., Sun, A., & Wang, R. (2021). Cold plasma jet with dielectric barrier configuration: Investigating its effect on the cell membrane of E. coli and S. cerevisiae and its impact on the quality of chokeberry juice. *Lwt, 136*, 110223. https://doi.org/10.1016/j.lwt.2020.110223

Huang, B., Zhao, K., Zhang, Z., Liu, F., Hu, H., & Pan, S. (2018). Changes on the rheological properties of pectin-enriched mango nectar by high intensity ultrasound. *Lwt, 91*(January), 414–422. https://doi.org/10.1016/j.lwt.2018.01.062

Igual, M., García-Martínez, E., Camacho, M. M., & Martínez-Navarrete, N. (2010). Effect of thermal treatment and storage on the stability of organic acids and the functional value of grapefruit juice. *Food Chemistry, 118*(2), 291–299. https://doi.org/10.1016/J.FOODCHEM.2009.04.118

Illera, A. E., Chaple, S., Sanz, M. T., Ng, S., Lu, P., Jones, J., Carey, E., & Bourke, P. (2019). Effect of cold plasma on polyphenol oxidase inactivation in cloudy apple juice and on the quality parameters of the juice during storage. *Food Chemistry, X, 3*. https://doi.org/10.1016/j.fochx.2019.100049

Kalaivendan, R. G. T., Eazhumalai, G., & Annapure, U. S. (2023). Impact of novel atmospheric pin-to-plate cold plasma on a seed galactomannan: Physical and chemical characteristics and its application in orange juice stabilization. *Food and Bioprocess Technology, 2023*(1), 1–19. https://doi.org/10.1007/S11947-023-03129-7

Karunanithi, S., Guha, P., & Srivastav, P. P. (2022). Cold plasma-assisted microwave pretreatment on essential oil extraction from betel leaves: Process optimization and its quality. *Food and Bioprocess Technology, 16*(3), 603–626. https://doi.org/10.1007/S11947-022-02957-3

Khodabandeh, M., Azizi, M., Shokri, B., Bahreini, M., Rezadoost, H., & Salehi, M. (2023). Optimization of the radiofrequency low-pressure cold plasma conditions for decontamination of saffrons. *Food and Bioprocess Technology, 1*, 1–27. https://doi.org/10.1007/S11947-023-03112-2/FIGURES/6

Khoshkalam Pour, A., Khorram, S., Ehsani, A., Ostadrahimi, A., & Ghasempour, Z. (2022). Atmospheric cold plasma effect on quality attributes of banana slices: Its potential use in blanching process. *Innovative Food Science and Emerging Technologies, 76*, 102945. https://doi.org/10.1016/j.ifset.2022.102945

Kumar, S., Pipliya, S., & Srivastav, P. P. (2023a). Effect of cold plasma processing on physicochemical and nutritional quality attributes of kiwifruit juice. *Journal of Food Science.* https://doi.org/10.1111/1750-3841.16494

Kumar, S., Pipliya, S., & Srivastav, P. P. (2023b). Effect of cold plasma on different polyphenol compounds: A review. *Journal of Food Process Engineering, 46*(1), e14203. https://doi.org/10.1111/JFPE.14203

Kumar, S., Pipliya, S., & Srivastav, P. P. (2023c). nth order kinetic modelling of peroxidase and polyphenol oxidase inactivation in kiwifruit juice during cold plasma and thermal treatment. *Innovative Food Science & Emerging Technologies, 103475.* https://doi.org/10.1016/J.IFSET.2023.103475

Landl, A., Abadias, M., Sárraga, C., Viñas, I., & Picouet, P. A. (2010). Effect of high pressure processing on the quality of acidified Granny Smith apple purée product. *Innovative Food Science and Emerging Technologies, 11*(4), 557–564. https://doi.org/10.1016/j.ifset.2010.09.001

Laorko, A., Tongchitpakdee, S., & Youravong, W. (2013). Storage quality of pineapple juice non-thermally pasteurized and clarified by microfiltration. *Journal of Food Engineering, 116*(2), 554–561. https://doi.org/10.1016/j.jfoodeng.2012.12.033

Li, J., Zhou, Y., & Lu, W. (2023). Enhancement of haskap vacuum freeze-drying efficiency and quality attributes using cold plasma pretreatment. *Food and Bioprocess Technology, 1*, 1–13. https://doi.org/10.1007/S11947-023-03186-Y/FIGURES/7

Liao, X., Li, J., Muhammad, A. I., Suo, Y., Chen, S., Ye, X., Liu, D., & Ding, T. (2018). Application of a dielectric barrier discharge atmospheric cold plasma (Dbd-Acp) for Eshcerichia Coli inactivation in apple juice. *Journal of Food Science, 83*(2), 401–408. https://doi.org/10.1111/1750-3841.14045

Manzoor, M. F., Hussain, A., Goksen, G., Ali, M., Khalil, A. A., Zeng, X. A., Jambrak, A. R., & Lorenzo, J. M. (2023). Probing the impact of sustainable emerging sonication and DBD plasma technologies on the quality of wheat sprouts juice. *Ultrasonics Sonochemistry, 92,.* https://doi.org/10.1016/j.ultsonch.2022.106257

Mehta, D., Yadav, K., Chaturvedi, K., Shivhare, U. S., & Yadav, S. K. (2022). Impact of cold plasma on extraction of polyphenol from de-oiled rice and corn bran: Improvement in extraction efficiency, in vitro digestibility, antioxidant activity, cytotoxicity and anti-inflammatory responses. *Food and Bioprocess Technology, 15*(5), 1142–1156. https://doi.org/10.1007/S11947-022-02801-8/FIGURES/6

Miguel, T. B. A. R., Porto, E. C. M., de Paiva Pinheiro, S. K., de Castro Miguel, E., Fernandes, F. A. N., & Rodrigues, S. (2021). Protective effect of natural and processed coconut water by non-thermal technologies against oxidative stress in brine shrimp (Artemia salina). *Food and Bioprocess Technology, 14*(4), 702–716. https://doi.org/10.1007/S11947-021-02600-7/FIGURES/9

Misra, N. N., Moiseev, T., Patil, S., Pankaj, S. K., Bourke, P., Mosnier, J. P., Keener, K. M., & Cullen, P. J. (2014). Cold plasma in modified atmospheres for post-harvest treatment of strawberries. *Food and Bioprocess Technology, 7*(10), 3045–3054. https://doi.org/10.1007/s11947-014-1356-0

Mol, S., Akan, T., Kartal, S., Coşansu, S., Tosun, ŞY., Alakavuk, D. Ü., Ulusoy, Ş, Doğruyol, H., & Bostan, K. (2023). Effects of air and helium cold plasma on sensory acceptability and quality of fresh sea bass (Dicentrarchus labrax). *Food and Bioprocess Technology, 16*(3), 537–548. https://doi.org/10.1007/S11947-022-02950-W/FIGURES/8

Mousavi, M., Hosseini, S. M., Hosseini, H., Abedi, A. S., Khani, M., Heshmati, A., Abhari, K., Shahraz, F., Taghizadeh, M., & Akhavan, A. (2022). Gliding arc plasma discharge conditions on microbial, physicochemical, and sensory properties of shrimp (Litopenaeus vannamei): In vivo and in vitro studies. *Food and Bioprocess Technology, 15*(10), 2327–2343. https://doi.org/10.1007/S11947-022-02886-1/FIGURES/7

Murtaza, A., Muhammad, Z., Iqbal, A., Ramzan, R., Liu, Y., Pan, S., & Hu, W. (2018). Aggregation and conformational changes in native and thermally treated polyphenol oxidase from apple juice (Malus domestica). *Frontiers in Chemistry, 6*, 1–10. https://doi.org/10.3389/fchem.2018.00203

Namjoo, M., Moradi, M., Dibagar, N., & Niakousari, M. (2022). Cold plasma pretreatment prior to ultrasound-assisted air drying of cumin seeds. *Food and Bioprocess Technology, 15*(9), 2065–2083. https://doi.org/10.1007/S11947-022-02863-8/FIGURES/9

Nasiru, M. M., Boateng, E. F., Alnadari, F., Umair, M., Wang, Z., Senan, A. M., Yan, W., Zhuang, H., & Zhang, J. (2023). Dielectric barrier discharge cold atmospheric plasma treatment of egg white protein: Insights into the functional, rheological, and structural properties. *Food and Bioprocess Technology, 2023*(1), 1–22. https://doi.org/10.1007/S11947-023-03159-1

Onal-Ulusoy, B. (2021). Effects of cold atmospheric gliding arc discharge plasma, non-thermal ultrasound, and low-temperature oven treatments on quality parameters of turkish blossom honey. *Food and Bioprocess Technology, 14*(9), 1763–1771. https://doi.org/10.1007/S11947-021-02688-X/FIGURES/1

Pankaj, S. K., Wan, Z., Colonna, W., & Keener, K. M. (2017). Effect of high voltage atmospheric cold plasma on white grape juice quality. *Journal of the Science of Food and Agriculture, 97*(12), 4016–4021. https://doi.org/10.1002/JSFA.8268

Pipliya, S., Kumar, S., & Srivastav, P. P. (2023a). Modeling of the inactivation kinetics of aerobic mesophiles and yeasts and molds natural microbiota in nonthermal plasma-treated pineapple (Ananas comosus) juice. *Journal of Food Science*, 1–15. https://doi.org/10.1111/1750-3841.16721

Pipliya, S., Kumar, S., & Srivastav, P. P. (2023b). Effect of dielectric barrier discharge nonthermal plasma treatment on physicochemical, nutritional, and phytochemical quality attributes of pineapple. *Journal of Food Science, 88*(11), 4403–4423. https://doi.org/10.1111/1750-3841.16767

Pipliya, S., Kumar, S., Babar, N., & Srivastav, P. P. (2023c). Recent trends in non-thermal plasma and plasma activated water: Effect on quality attributes, mechanism of interaction and potential application in food & agriculture. *Food Chemistry Advances, 2*, 100249. https://doi.org/10.1016/J.FOCHA.2023.100249

Pipliya, S., Kumar, S., & Srivastav, P. P. (2022). Inactivation kinetics of polyphenol oxidase and peroxidase in pineapple juice by dielectric barrier discharge plasma technology. *Innovative Food Science & Emerging Technologies, 80*, 103081. https://doi.org/10.1016/J.IFSET.2022.103081

Ranganna, S. (2007). *Handbook of analysis and quality control for fruit and vegetable products* (pp. 9–10 (105–6)). New Delhi: Tata McGraw-Hill Publishing Co. Ltd.

Rashvand, M., Matera, A., Altieri, G., Genovese, F., Nikzadfar, M., Feyissa, A. H., & Di Renzo, G. C. (2023). Effect of dielectric barrier discharge cold plasma on the bio-nanocomposite film and its potential to preserve the quality of strawberry under modified atmosphere packaging. *Food and Bioprocess Technology, 1*, 1–18. https://doi.org/10.1007/S11947-023-03196-W/FIGURES/7

Rodrigues, S., & Fernandes, F. A. N. (2023). Effect of dielectric barrier discharge plasma treatment in pasteurized orange juice: Changes in volatile composition, aroma, and mitigation of off-flavors. *Food and Bioprocess Technology, 16*(4), 930–939. https://doi.org/10.1007/S11947-022-02976-0/FIGURES/4

Rodriguez, Ó., Rodrigues, S., & Fernandes, F. A. N. (2022). Effect of glow discharge plasma technology on the phenolic content and antioxidant capacity of four tropical juices with different phenolic composition. *Journal of Food Processing and Preservation, 46*(1), e16110. https://doi.org/10.1111/JFPP.16110

Sangwanna, S., Seelarat, W., Panklai, T., Chaosuan, N., Subcharoen, A., Subcharoen, N., Chanchula, N., Inyod, T., Toemarrom, T., Bootchanont, A., Wattanawikkam, C., Pavasupree, S., Boonyawan, D., & Porjai, P. (2023). Air atmospheric pressure plasma jet to improve fruiting body production and enhance bioactive phytochemicals from mutant Cordyceps militaris (White Cordyceps militaris). *Food and Bioprocess Technology, 16*(9), 1976–1991. https://doi.org/10.1007/S11947-023-03028-X/TABLES/3

Segat, A., Misra, N. N., Cullen, P. J., & Innocente, N. (2016). Effect of atmospheric pressure cold plasma (ACP) on activity and structure of alkaline phosphatase. *Food and Bioproducts Processing, 98*, 181–188. https://doi.org/10.1016/j.fbp.2016.01.010

Sew, C. C., Mohd Ghazali, H., Martín-Belloso, O., & Noranizan, M. A. (2014). Effects of combining ultraviolet and mild heat treatments on enzymatic activities and total phenolic contents in pineapple juice. *Innovative Food Science & Emerging Technologies, 26*, 511–516. https://doi.org/10.1016/J.IFSET.2014.05.008

Sharma, S., Prabhakar, H., & Singh, R. K. (2022). Atmospheric cold plasma-induced changes in milk proteins. *Food and Bioprocess Technology, 15*(12), 2737–2748. https://doi.org/10.1007/S11947-022-02915-Z/TABLES/5

Shevkani, K., Singh, N., Kaur, A., & Rana, J. C. (2015). Structural and functional characterization of kidney bean and field pea protein isolates: A comparative study. *Food Hydrocolloids, 43*, 679–689. https://doi.org/10.1016/j.foodhyd.2014.07.024

Silva, R. M., Filho, E. G. A., Campelo, P. H., Silva, F. E. F., Zampieri, D. S., Gramosa, N. V., Fernandes, F. A. N., & Rodrigues, S. (2022). NMR spectroscopy and chemometrics to evaluate the effect of different non-thermal plasma processing on Sapota-do-Solimões (Quararibea cordata Vischer) juice quality and composition. *Food and Bioprocess Technology, 15*(4), 875–890. https://doi.org/10.1007/S11947-022-02792-6/TABLES/4

Smelt, J. P. P. M., & Brul, S. (2014). Thermal inactivation of microorganisms. *Critical Reviews in Food Science and Nutrition, 54*(10), 1371–1385. https://doi.org/10.1080/10408398.2011.637645

Sruthi, N. U., Josna, K., Pandiselvam, R., Kothakota, A., Gavahian, M., & Mousavi Khaneghah, A. (2022). Impacts of cold plasma treatment on physicochemical, functional, bioactive, textural, and sensory attributes of food: A comprehensive review. *Food Chemistry, 368*, 130809. https://doi.org/10.1016/j.foodchem.2021.130809

Suo, G., Zhou, C., Su, W., & Hu, X. (2022a). Effects of ultrasonic treatment on color, carotenoid content, enzyme activity, rheological properties, and microstructure of pumpkin juice during storage. *Ultrasonics Sonochemistry, 84*(February), 105974. https://doi.org/10.1016/j.ultsonch.2022.105974

Suo, G., Zhou, C., Su, W., & Hu, X. (2022b). Effects of ultrasonic treatment on color, carotenoid content, enzyme activity, rheological properties, and microstructure of pumpkin juice during storage. *Ultrasonics Sonochemistry, 84*(March), 105974. https://doi.org/10.1016/j.ultsonch.2022.105974

Surowsky, B., Fischer, A., Schlueter, O., & Knorr, D. (2013). Cold plasma effects on enzyme activity in a model food system. *Innovative Food Science and Emerging Technologies, 19*, 146–152. https://doi.org/10.1016/j.ifset.2013.04.002

Tiwari, B. K., Muthukumarappan, K., O'Donnell, C. P., & Cullen, P. J. (2008). Kinetics of freshly squeezed orange juice quality changes during ozone processing. *Journal of Agricultural and Food Chemistry, 56*(15), 6416–6422. https://doi.org/10.1021/JF800515E/ASSET/IMAGES/LARGE/JF-2008-00515E_0006.JPEG

Vivek, K., Subbarao, K. V., Routray, W., Kamini, N. R., & Dash, K. K. (2020). Application of fuzzy logic in sensory evaluation of food products: A comprehensive study. *Food and Bioprocess Technology, 13*(1), 1–29. https://doi.org/10.1007/s11947-019-02337-4

Wang, J., Vanga, S. K., & Raghavan, V. (2019). High-intensity ultrasound processing of kiwifruit juice: Effects on the ascorbic acid, total phenolics, flavonoids and antioxidant capacity. *LWT, 107*, 299–307. https://doi.org/10.1016/J.LWT.2019.03.024

Wang, J., Zhuang, H., & Zhang, J. (2016). Inactivation of spoilage bacteria in package by dielectric barrier discharge atmospheric cold plasma—Treatment time effects. *Food and Bioprocess Technology, 9*(10), 1648–1652. https://doi.org/10.1007/s11947-016-1746-6

Wang, X., Han, Y., Niu, H., Zhang, L. H., Xiang, Q., & Zong, W. (2022). Alternaria mycotoxin degradation and quality evaluation of jujube juice by cold plasma treatment. *Food Control, 137*(February), 108926. https://doi.org/10.1016/j.foodcont.2022.108926

Wang, Y., Wang, Z., Zhu, X., Yuan, Y., Gao, Z., & Yue, T. (2020). Application of electrical discharge plasma on the inactivation of Zygosaccharomyces rouxii in apple juice. *LWT, 121*, 108974. https://doi.org/10.1016/J.LWT.2019.108974

Wei, K., & Ren, B. (2018). A method on dynamic path planning for robotic manipulator autonomous obstacle avoidance based on an improved RRT algorithm. *Sensors (Switzerland), 18*(2). https://doi.org/10.3390/s18020571

Wu, D., Forghani, F., Daliri, E. B. M., Li, J., Liao, X., Liu, D., Ye, X., Chen, S., & Ding, T. (2020). Microbial response to some nonthermal physical technologies. *Trends in Food Science & Technology, 95*, 107–117. https://doi.org/10.1016/J.TIFS.2019.11.012

Wu, Y., Cheng, J. H., Keener, K. M., & Sun, D. W. (2023). Inhibitory effects of dielectric barrier discharge cold plasma on pathogenic enzymes and anthracnose for mango postharvest preservation. *Postharvest Biology and Technology, 196*, 112181. https://doi.org/10.1016/J.POSTHARVBIO.2022.112181

Wurlitzer, N. J., Dionísio, A. P., Lima, J. R., dos Garruti, D., & S., Silva Araújo, I. M. da, da Rocha, R. F. J., & Maia, J. L. (2019). Tropical fruit juice: Effect of thermal treatment and storage time on sensory and functional properties. *Journal of Food Science and Technology, 56*(12), 5184–5193. https://doi.org/10.1007/s13197-019-03987-0

Xu, L., Garner, A. L., Tao, B., & Keener, K. M. (2017). Microbial inactivation and quality changes in orange juice treated by high voltage atmospheric cold plasma. *Food and Bioprocess Technology, 10*(10), 1778–1791. https://doi.org/10.1007/S11947-017-1947-7/FIGURES/8

Xu, L., Yepez, X., Applegate, B., Keener, K. M., Tao, B., & Garner, A. L. (2020). Penetration and microbial inactivation by high voltage atmospheric cold plasma in semi-solid material. *Food and Bioprocess Technology, 13*(10), 1688–1702. https://doi.org/10.1007/s11947-020-02506-w

Zielinska, S., Cybulska, J., Pieczywek, P., Zdunek, A., Kurzyna-Szklarek, M., Staniszewska, I., Liu, Z. L., Pan, Z., Xiao, H. W., & Zielinska, M. (2022). Structural morphology and rheological properties of pectin fractions extracted from okra pods subjected to cold plasma treatment. *Food and Bioprocess Technology, 15*(5), 1168–1181. https://doi.org/10.1007/S11947-022-02798-0/FIGURES/3

Ziuzina, D., Patil, S., Cullen, P. J., Keener, K. M., & Bourke, P. (2014). Atmospheric cold plasma inactivation of Escherichia coli, Salmonella enterica serovar Typhimurium and Listeria monocytogenes inoculated on fresh produce. *Food Microbiology, 42*, 109–116. https://doi.org/10.1016/j.fm.2014.02.007